N° d'ordre :
N° de série :

DEMOCRATIC AND POPULAR REPUBLIC OF ALGERIA
MINISTRY OF HIGHER EDUCATION AND SCIENTIFIC RESEARCH

UNIVERSITY CENTER OF EL-OUED
INSTITUTE OF SCIENCE AND TECHNOLOGY
Department of Electronics

Dissertation Presented
For Graduation of:

ACADEMIC Master

Domain: **Sciences and Techniques**
Sector: **Electronics**
Specialty: **Telecommunications**

Presented by: **HASSANI Bilal**

Study of the linear effects of Photonic Crystal Fiber (PCF)

Date of dissertation: 27 / 06 / 2012

In front of jury composed of:

M.	**Ferhat REHOUMA**	Pr	President
M.	**Abdellatif MAMANOU**	M.A.A	Examiner
M.	**Saïd MEHELLOU**	M.A.B	Examiner
M.	**Abdelkader MEDJOURI**	M.A.A	Reporter

2011-2012

Abstract

In recent years, one of the most dynamically developing branches of fiber optics is photonic crystal fiber which is made of single pure silica with an arrangement of micro air holes over the cladding region. The propagation of light in these structures can be acheived by two different mechanisms: total internal reflection and the photonic bandgap effect (PBG). Linear properties, that characterize any optical waveguide, such as endlessly single modeness, confinement loss, chromatic dispersion, and the birefringence are studied by varying the structural parameters. Aiming to achieving a perfect light propagation with specific purposes (HI-BI), different patterns of photonic crystal fiber are analyzed using the well known FDTD method.

Keywords: *photonic crystal fiber, effective index, high birefringence, chromatic dispersion, confinement loss, FDTD method.*

Résumé

Au cours des dernières années, la fibre à cristaux photoniques est l'une des branches dynamiques les plus développées dans le domaine optique, cette fibre est fabriquée de la silice pure avec un arrangement de trous d'air micrométrique au niveau de la gaine. La propagation de la lumière dans ces structures peut être atteinte par deux mécanismes différents: la réflexion totale interne et avec l'effet à bande interdite photonique (BIP). Des propriétés linéaires, qui caractérisent chaque guide d'onde optique, comme la caractéristique d'infiniment monomode, la perte par confinement, la dispersion chromatique et la biréfringence sont étudiées en variant leurs paramètres géométriques. Dans le but d'obtenir une propagation parfaite de lumière avec des objectifs spécifiques (HI-BI), différents patterns de fibre à cristaux photoniques sont analysés en utilisant la méthode bien connue FDTD.

Mots clés: *fibre à cristaux photoniques, indice de réfraction effective, haut biréfringence, dispersion chromatique, perte par confinement, la méthode FDTD*

Contents

List of Figures

List of Abbreviations

PCF	**Photonic Crystal Fiber**
TIR	**Total Internal Reflection**
PMD	**Polarization Mode Dispersion**
FEM	**Finite Element Method**
PWEM	**Plane Wave Expansion Method**
FDTDM	**Finite Difference Time Domain Method**
PhCs	**Photonic Crystals**
Hi-Bi	**High Birefringence**
FCC	**Face Centered Cubic**
1D, 2D, 3D	**One, Two, Three Dimensional Photonic Crystals**
PBG	**Photonic Band Gap**
TMM	**Transfer Matrix Method**
MPB	**MIT Photonic Band Gap**
TE	**Transverse Electric**
TM	**Transverse Magnetic**
GLAD	**Glancing Angle Deposition**
SMF	**Single-Mode Fiber**

HCPCF	Hollow Core Photonic Crystal Fiber
LED	Light Emission Diode
ZWE	Zero Wavelength Dispersion
LPG	Long Period Grating
LMA	Large Mode Area
FTM	Finite Time Method
ESM	Endlessly Single-Mode
DF	Dispersion Flattened
PP-PCF	Pseudo-Panda PCF

Introduction

Over the past years and since the existence of mankind, human beings were always endeavouring to contact each other, especially, those who were far away from them. Taking a historical view, this contact started with traditional signs such as flames and sun rays, then gradually changed to Carrier pigeon and Morse code, until it reached today's developed phones. Recently, and precisely after the scientific revolution, the operation of communication has become rather easy and more effective. Notwithstanding the evolution of mobile's communication, the necessity to wires still strongly exists. The technological development is, steadily, showing a great necessity to transmit huge information during short periods of time. Simultaneously, the copper cables proved their inability for such transmission because of the small available bandwidth, the electromagnetic interferences and the high tension needed for this operation, in addition to their inability for heavy weight... etc. The solution was in the optical fiber. This medium was the result of many works: from the early experiments by John Tyndall in the guided transmission light, and the photophone of Alexander Graham Bell, passing by the development of light emitting diodes and lasers, to the well known fused silica optical waveguide fiber in 1970. This cable had played a significant role in the world of telecommunications thanks to its huge bandwidth. The latter allows to transmit giga of bits over long distances at a very short time (speed of light) with less loss, and also immune the electromagnetic interferences. Moreover, it is done with a tiny size. Yet, the progression of science and man's desire for perfection has made it possible for another design of optical fiber to be brought to light. This fiber known as microstructured optical fiber or the photonic crystal fiber has proved to reduce the existing counted disadvantages. Classical optical fibers perform very well in telecom and non-telecom applications, but there is a series of fundamental limits related to their structures. The fibers have rigid design rules to fulfill: limited core diameter in the single-mode regime, modal cut-off wavelength, limited material choice (thermal

properties of core glass and cladding glass must be the same). The idea to prepare photonic crystal fibers (PCF), as their name show, goes back to the birth of photonic crystals. The ability to tailor structures on the micro and nano-scale range, in the late 1980s, provided the opportunity to investigate the relation between the structure of matter and light. Three dimensional photonic crystal structures are periodic, dielectric structures in which light may behave similar way as electron waves in a crystal lattice. Photonic crystal fiber geometry is characterized by a periodic arrangement of air holes running along the entire length of the fiber, centered on a solid or hollow-core. The major difference between both kinds of fibers relies on the fact that the PCF properties are not from spatially varying glass composition, as in conventional optical fiber, but from an arrangement of very tiny and closely spaced air holes which go through the whole length of fiber. In contrast with standard optical fibers, photonic crystal fibers can be made of a single material and have several geometric parameters which can be manipulated offering large flexibility of design: lattice pitch, air hole shape and diameter, refractive index of the glass, and type of lattice. Light can propagate according to two mechanisms: the modified total internal reflection (TIR), which is very similar to the one in conventional fibers, since the solid core index is higher than the cladding index due the existence of the air holes. The second mechanism is based on a photonic band gap created as a result of the periodic structure in the cladding region which makes a forbidden propagation of light for a specific wavelength range.

The photonic crystal fiber has since it was first proposed attracted growing attention due to its many unique properties. One of the first special characteristics to be reported for the PCF was its potential to be endlessly single-mode (ESM) referring to the absence of higher-order modes regardless of the optical wavelength. By manipulating the structure, it is possible to design desired dispersion properties of the fiber. PCFs having zero, low, or anomalous dispersion at visible wavelengths can be designed and fabricated. The dispersion can also be flattened over a very large range. High birefringence can be easily achieved with photonic crystal fibers by introducing, deliberately, a uniform and asymmetrical stress. It can be used to compensate the polarization mode dispersion (PMD), to achieve optical filters, fiber lasers, and fiber sensors. Due to the complex structure of a PCF, different numerical techniques have been used to study the different properties of this fiber, such as the finite element method (FEM) and the plane wave expansion method (PWEM). Among these methods, finite difference time domain method (FDTDM) is one of the best methods for calculating different propagation properties of a fiber. Both the real and imaginary parts of the modal indices are essential parameters. The real part of the modal indices determines among others, the dispersion properties, while the imaginary part determines the confinement loss. The confinement loss is an important parameter to discriminate one mode from the others;

hence, one can have structures with wide effectively-single-mode operation wavelength range or non-polarization-degenerate effectively-single-mode operation. Therefore, the ability to calculate both the real and imaginary part of the modal indices is important.

These papers are structured to study the linear effects of the solid core microstructured optical fiber air/silica:

The first chapter is about the physics of photonic crystals. It talks about the evolution of the PhC over the years, and then it discusses in general the three main types: one, two, and three dimensional photonic crystals. This second type was the idea that permits the photonic crystal fiber to see light.

The second chapter gives an overview about the photonic crystal fiber, staring with historical notes and the geometric design, and then discovering its optical properties, finishing with some of its huge applications, and how PCF can be fabricated.

The optical proprieties of the photonic crystal fiber are studied by simulation in the third chapter. The endlessly single mode, the confinement loss, the chromatic dispersion and the birefringence are discussed using different structures and geometric parameters.

The last chapter focuses in one from the most important applications of the PCF which is the high birefringence (HI-BI). Two structures for four different types are investigated. The study is performed according to three criterions: the birefringence, the chromatic dispersion and the confinement loss.

Chapter 2

The photonic crystals

2.1 Introduction

A crystal is a periodic arrangement of atoms or molecules. If a small basic building block of atoms or molecules is repeated spatially, a crystal lattice will be formed. As is well known, semiconductor materials have a bandgap between the valence and conduction energy bands. Electrons are forbidden to occupy any energy level within the bandgap. Similarly, if the dielectric constant of a material changes periodically in space, the material is referred to as a photonic crystal. A photonic crystal possesses a forbidden frequency band in which propagation of electromagnetic waves is prohibited. According to the number of directions in which dielectric materials exhibit periodicity, one-, two-, or three-dimensional photonic crystal structures are possible. Scattering of light by photonic crystals can produce many of the analogous phenomena for photons to the atomic potential acting on electrons.

Photonic crystal structures are analogous to normal crystals in which atoms or groups of atoms are arranged in a repeating pattern, except that the repeat period is on the order of a micron rather than a fraction of a nanometer. In 1987, Yablonovitch suggested an application of photonic crystals in semiconductor lasers in order to control the spontaneous emission [1]. This was based on the idea that a photonic structure can be designed to introduce a frequency bandgap coinciding with the spectrum of the spontaneous emission. Other scientists have proposed applications of photonic crystal structures at millimeter and microwave frequencies in order to achieve desired performances for waveguides [2].

2.2 Historical overview

Now, we can briefly consider the PhCs' evolution as well as methods for their design and investigation.

In spite of the fact that PhCs have attracted high attention only during the last several decades, first assumptions of possibility to control the light propagation using the periodic structures relate to 1887 [3]. Those were the investigations of 1D periodic structures.

Almost after 100 years in 1972, Soviet Union scientist V.P. Bykov published a paper where he described the possibility to use periodic structures for the spontaneous emission control [4].

However, the first works assumed to start the intensive progress of PhC are the works of E.Yablonovitch and S. John which was issued in 1987 in Physical Review Letters [5] [6]. Papers are dedicated to the possibility of spontaneous emission management as well as the possibility of the radiation propagation control using periodic structures. After publication of these articles, a number of publications dedicated to PhC physics and technology doubles every year. In 1990, K.M. Ho, C.T. Chan and C.M. Soukoulis [7] obtained the band structure of the PhC with FCC lattices (opal structure) which consisted of dielectric spheres with high refractive index placed in air.

In 1992, H.S. Sozuer and J.W. Haus [8] computed the band structure of the PhC with inverted FCC lattice (also known as inverted opal) .The term inverted opal means that instead of dielectric spheres placed in air, the inverted FCC lattice consists of a number of spherical cavities separated by baffles with higher refractive index (see figure 2.1).It appeared that such a PhC has complete PBG at relatively high refractive index of material. Investigated inverted opal had complete PBG between the eighth and ninth bands.

The appearance of the complete PBG inside the PhC with inverted FCC lattice attracts a special interest, because today inverted artificial opals provide possibility of mass PhC production.

In 1998, the inverted artificial opal was obtained experimentally [9]. The sphere's diameter in the structure was approximately 1 μm, and the distance between the spheres is very low so the spheres are almost touching. From the technological point of view, it is much easier to grow the structure with such parameters than with high distance between spheres because the base FCC lattice consists of dielectric spheres in air so when the spheres touch each other, their position can be easily locked in. The refractive index of the PhC material between spheres (TiO2) is 2.8 and it is too small to form the complete PBG. However, when silica is used as the bulk material,

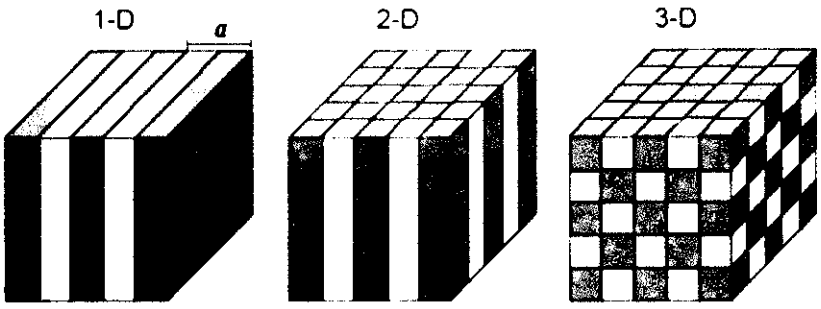

Figure 2.1: schematics of a 1D, 2D and 3D photonic crystal. The colours represent materials with different dielectric indices. The spatial period of the material is called the lattice constant, a

the appearance of the complete PBG is possible at some geometric parameters.

In 2000, the first 3D PhC which had the complete PBG within near infrared range was obtained [10]. Such a PhC consisted of silicon spheres arranged in a diamond lattice.

Starting from 1987 and till 2005 more than 10,000 printed works dedicated to PhCs and PhC-based devices were published. However, the serial production now is available only for microstructured fibers which possess unique properties and the possibility to manage the parameters and characteristics within wide range and 1D PhCs which are produced in the form of distributed Bragg reflectors of vertical cavity surface emitting lasers or in form in the form of fiber Bragg gratings.

Schematic pictures of one-, two- and three-dimensional (1D, 2D and 3D) PCs are presented in figure 2.1 where the high- and low-index materials are shown in red and yellow, respectively.

2.3 One-dimensional structures

Pedagogically, a 1D well structure where the optical wavelength of each segment corresponding to one optical quarter wavelength thick, $\lambda/4$, serves as a useful pedagogical starting point for understanding how a PC operates (figure 2.2)[11]. These types of structures were actually first discussed by Lord Rayleigh as early as 1887 [12].

The dielectric constant $\varepsilon(x)$ can be written as

$$\varepsilon(x) = \varepsilon_0 + \varepsilon(x) \tag{2.1}$$

Where ε_0 is the average dielectric constant and $\varepsilon(x)$ represents the spatial vari-

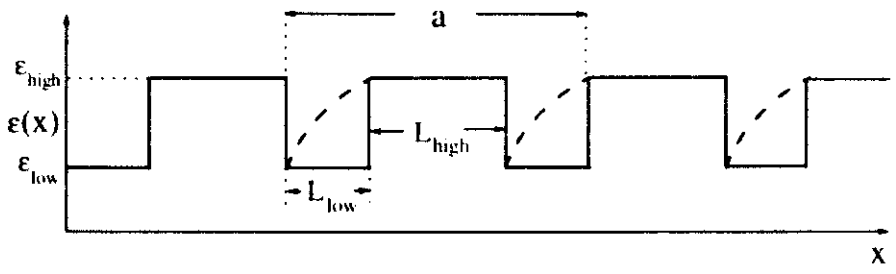

Figure 2.2: A one-dimensional square-well constant potential with periodicity, a, and low- and high-index thicknesses within the unit cell $=L_{low}$ and L_{high}, respectively. Such a system undergoes Bragg scattering. The dashed line within the low index well indicates a quarter wavelength which is the wavelength dimension that would be required for maximum reflectivity

ation of $\varepsilon(x)$. The index of refraction, n, in the absence of absorption, is related to the dielectric constant through the relation $n = \sqrt{k}$. The total dielectric constant is assumed to be real and positive everywhere in space. Assume that the lattice periodicity has the dimension 'a', and that the low-index and high-index segment thicknesses are L_{low} and L_{high}, respectively. Thus, the periodicity $a = L_{low} + L_{high}$. The optical thickness of each segment is given by the product of the geometrical distance involved and the index of refraction.

Two synergistic optical scattering phenomena can occur within such a periodic arrangement. The first is Bragg scattering which will occur when the overall geometric periodicity of the repeating structure is an integer multiple of half the optical wavelength, that is, when

$$m\lambda/2 = a \tag{2.2}$$

Where m is an integer, $m = \pm 1, \pm 2, \pm 3, ..$

The second is reflection within each unit cell which will be a maximum when the segment optical thicknesses equal one quarter optical wavelength, that is, when:

$$n_{high} L_{low} = n_{low} L_{low} = \lambda/4 \tag{2.3}$$

A 'stop band' or 'band gap' will open when the dimensions of the periodicity and the segments are chosen so that both scattering conditions occur at the same wavelength. Constructive interference of the multiple reflected rays will then maximize

the overall reflection of the material. Generally, the periodic arrangement of different dielectric materials opens a gap in one dimension. The width of the stop band or band gap is an increasing function of the index of refraction (or dielectric constant) ratio of the high and low-index materials. It can be shown that at normal incidence the edges of the stop gap centered at frequency ω_0 occur at $\omega_0 \pm \Delta\omega$ where:

$$\frac{\Delta\omega}{\omega_0} = \frac{2}{\pi}\arcsin\left(\frac{n_{high} - n_{low}}{n_{high} + n_{low}}\right) \tag{2.4}$$

and are independent of light polarization [13]. At other angles the reflectivity becomes polarization dependent.

The effects described above also arise in other well-established techniques which involve Bragg scattering such as x-ray diffraction. One may then be tempted to ask why the concept of photonic crystals has achieved such prominence in recent years. Indeed, is the moniker 'photonic crystal' simply a new name for an old phenomenon? This question was recently addressed by Yablonovitch who suggested that the name photonic crystals should apply only to 2D and 3D periodic structures with a large dielectric contrast (>2) [14] which is defined as the ratio of the dielectric constants of the high and low ε-regions, that is, ε_{high} /ε_{low}. That said, many publications appear yearly on the subject of 1D PCs.

Some of the approaches used to calculate band structures include the plane wave expansion method (PWEM) [15], the transfer matrix method (TMM) [16][17] and the finite difference time domain method (FDTD) [18].

The band diagram shown in figure 2.3 is generated by MIT photonic band gap (MPB) software. This software based on the PWEM is a free software package developed for Unix systems by S. G. Johnson and the Joannopoulos Ab Initio Physics group at MIT.

A typical plot of normalized photon frequency ($= \omega a/2\pi$) versus wave vector (photonic band structure) for a high index contrast 1D dielectric stack is shown for a range of wave vector $\vec{k}$-values ($\vec{k} = 2\pi/\lambda$) between -π/a and π/a

2.4 Natural photonic crystals

Although PC architectures appear to be artificial, they are actually found in naturally occurring opal gemstones, and in many living organisms [19][21]. Species that exhibit iridescent colours due to interference effects include the peacock, comb-jellyfish, the sea mouse, the rainforest beetle and the blue Morpho butterfly. Although widely cited as an example of a natural photonic crystal, the Morpho butterfly is perhaps not actually prototypical because its coloration is thought to involve both interference and

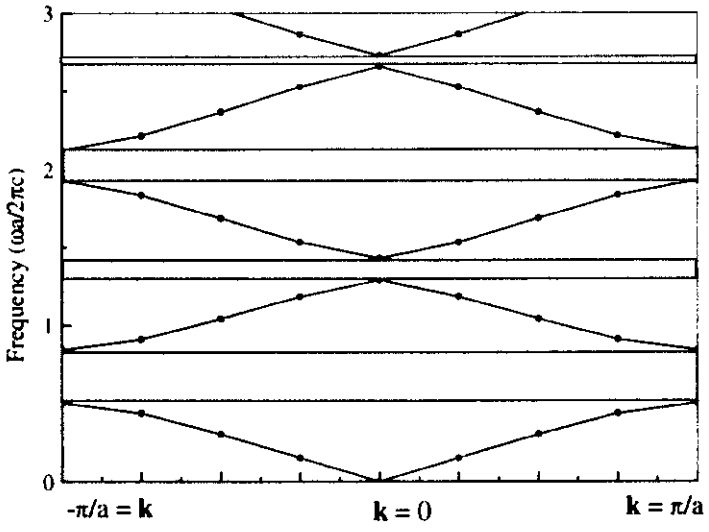

Figure 2.3: Band structure for a multilayer dielectric stack of equal width with n_{low} = 2.9 and n_{high} = 6.7. The grey regions correspond to photonic band gaps. The first band gap is centred at 677 nm when a = 1μm. The band diagram is generated by MIT photonic band gap (MPB)

diffraction effects, and dye pigmentation [21]. Biologically, it is believed that species have evolved colour through Bragg reflections as a means of thermal regulation and signalling [22].

Naturally occurring periodic structures have almost exclusively 2D and 3D geometries, but are not, by the Yablonovitch criteria, genuine PCs because their dielectric contrasts are not particularly large. Their activity however can be explained by the extremely large number of periods found in these structures.

This allows them to behave as essentially infinite PCs which lead to perfect band gaps. The current goal experimentally is to fabricate in the lab what has been done in Nature over millions of years.

Semiconductor crystals analogies

The presence of a photonic band gap in a PC is also often described as the optical analogue of the electronic band gap associated with a semiconductor crystal. The periodic potential of the semiconducting crystal introduces gaps into the energy band structure along certain directions where electron waves are forbidden to propagate because of Bragg reflection. This is shown qualitatively in a plot of the electron energy versus electron wave vector $\vec{k}$ (figure 2.4). Note that the momentum of an

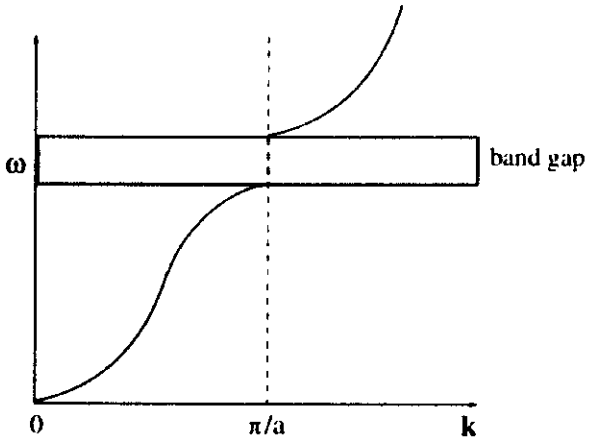

Figure 2.4: A plot of electron frequency, ω versus wave vector, $\vec{k}$ for a one-dimensional

electron is given by $\bar{\mathrm{h}}\vec{k}$ while its energy = $\bar{h}\omega$. In a 1D semiconductor the first Bragg reflection takes place in k- (reciprocal) space at k= $\pm\pi/a$

, where a is the periodicity of the lattice. The region in k-space between $-\pi/a$ and $+\pi/a$ is called the first Brillouin zone of the lattice, and stop gaps will occur at any positive or negative integer multiple of π/a.

By symmetry, the curve for negative values of k is simply the mirror image of this plot through a plane containing the $E-$axis at $k = 0$. These symmetry properties show that the dispersion plot for the 1D PC in figure 2.3 shows band gap effect similar to that in figure 2.4 . In a semiconductor, Bragg reflections at the periodic potentials produce standing waves of the electron wave function at the periodicity of the positively charged ion cores. Two standing waves are produced: one with its peak wave function amplitude occurring at the periodic potential maximum and one with its peak at the minimum [23]. This corresponds to two distinct energy levels with no available states in between, that is, a band gap. The energy state below the band gap is called the valence band, while the upper level is the conduction band.

Similarly, the energy levels below and above a photonic band gap correspond to electromagnetic standing waves with their energy maxima located in either the high or low dielectric regions. The regions of low dielectric constant is often filled with air which has $\varepsilon = 1$. Thus, it is common to label the region of lower dielectric constant the air band, even if the material involved is not air. The dielectric and air bands are the photonic analogues of the valence and conduction bands, respectively (figure 2.5). When the dielectric contrast in a PC is large, both standing waves actually have

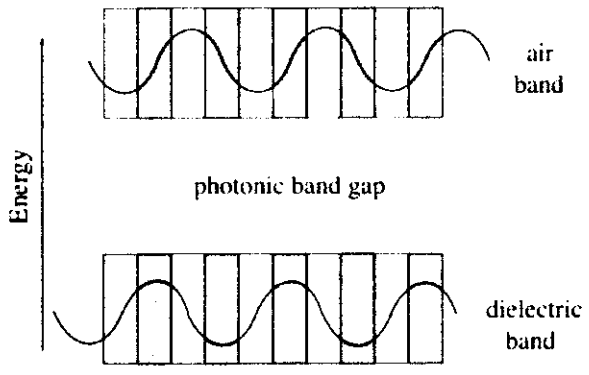

Figure 2.5: Schematic diagram of the field distributions in a 1D PC. The low-index segments are

their energy primarily in the high $\varepsilon-$layers, but with more energy concentrated in the bottom band, gaps form due to this difference in field energy location.

2.5 Two-dimensional photonic crystals

2D PCs are periodic in two directions and homogenous in the third. By symmetry, an electromagnetic wave propagating, for example, in the $xy-$plane of a 2D PC can be classified as transverse electric (TE) or transverse magnetic (TM) depending on their reflection symmetry through the xy -plane. TE modes have their H -vector perpendicular to the plane in the $z-$direction and their $E-$vector in the $xy-$plane. Conversely, TM modes have their $E-$vector perpendicular to the plane, and their $H-$vector in the $xy-$plane. 2D PCs are more complicated than 1D structures because their photonic responses are different for these two different polarizations. They can reflect light however from any direction in the plane unlike 1D PCs which only reflect light at normal incidence.

Highly symmetrical 2D PC geometries are usually either square or hexagonal [19]. It is common to label the direction of light propagation in a photonic band structure diagram.

Analysis shows that for square column array of high-index dielectric islands a photonic band gap will open between the first (dielectric) band and the second (air) band for the TM modes but not for the TE modes (figure 2.6).

Physically, this happens because the lowest TM mode is localized in the high

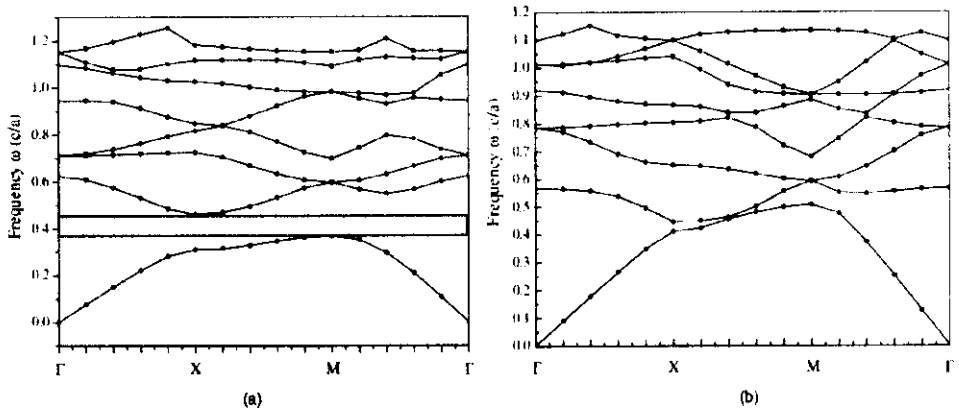

Figure 2.6: (a) Photonic band diagram for the TM modes. The grey box indicates the photonic band gap. (b) Photonic band diagram for the TE modes which do not exhibit a photonic band gap.

dielectric regions while most of the electromagnetic power of the air band is found in the low-ε regions. This result can be related to the fill factor which is a measure of the electric field intensity in the high dielectric region. This parameter is relatively large for TM modes but not for TE modes in a square column array lattice. On the other hand, if the square lattice is a grid of dielectric veins versus isolated air islands, the fill factors are reversed and it is the TE modes which exhibit a band gap.

A 'compromise' lattice of a high dielectric material can be created that is nearly isolated yet also connected (figure 2.7(a)) [24]. Specifically, a hexagonal lattice of air holes placed inside the high-index material creates an array of triangular high ε-spots connected by narrow veins. Figure 2.7(b) shows the resultant photonic band diagram calculated for a structure with a dielectric contrast = 6.7. A photonic band gap and hence complete reflection is found for both the TE and TM modes. Conversely, a hexagonal array of isolated high-index columns exhibits a band gap for the TM modes only, in line with the rule of thumb mentioned above.

The size of the photonic band gap can be characterized by the gap–midgap ratio which is defined as ω where ω is the gap frequency width and ω_0 is the frequency at the middle of the gap. This parameter which is typically of the order of 0.2 is more meaningful than ω alone as a measure of the size of the band gap since it is invariant to size scaling.

The size of band gap is affected by many parameters including the structural symmetry of the crystal, the dielectric constant ratio, the air-filling ratio and so on. Although it is difficult to provide a quantitative formula to describe the relationships

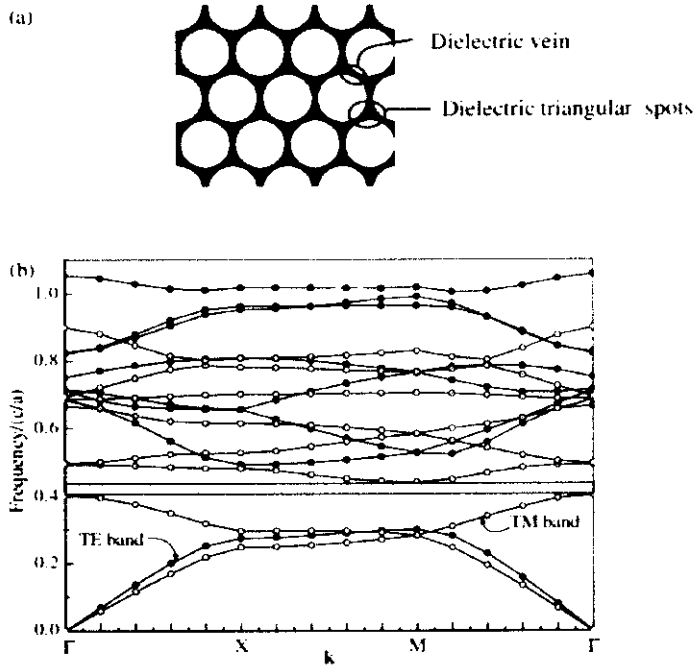

Figure 2.7: (a) A 2D triangular photonic crystal with a complete band gap for both TE and TM modes. The structure is a column array of air holes ($\varepsilon_{low} = 1$) in a dielectric substrate ($\varepsilon_{high} = 6.7$),

between these parameters, the size of the gap can be calculated provided the structure is symmetrical. For example, it can be shown that the photonic band gap disappears for the structure shown in figure 2.7(a) when the dielectric constant ratio = 4.

2.6 Three-dimensional photonic crystals

The first experimental realization of a 3D PC was achieved by Yablonovitchet al who fabricated a face centred cubic (fcc or opal-like) crystal in a low-loss dielectric medium, with a band gap operating in the microwave, by mechanically drilling tens of thousands of holes with radii slightly larger than close packing so that the voids joined up to form a connected network [25]. That system is known as the three cylinder structure or simply Yablonovite in recognition of this achievement.

The drilling angles along the three equivalent (110) directions used to generate Yablonovite are shown in figure 2.8 [26]. Both Yablonovite and its inverse structures are found to possess a complete band gap in three dimensions.

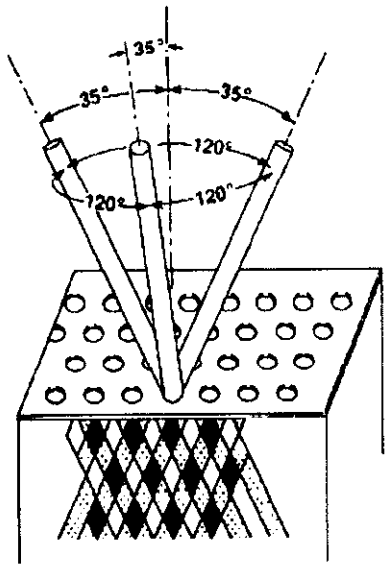

Figure 2.8: Drilling angles used to make Yabolonvite

One structure which is predicted to have a large complete band gap is a 3D diamond lattice of spheres [15]. Band gaps have been found for other structures including the simple cubic [27] and the rhombohedral A7 lattice [40] lattices. It was shown that the largest gap–midgap ratio (0.46) can be achieved for an inverse diamond lattice of overlapping air holes in a dielectric with a filling fraction = 0.81. Physically, this corresponds to 3D PC made essentially of air voids with an ultrathin dielectric skeleton framework. Coupled with the fact that visible reflections require submicron periodicities, it is hardly surprising that fabrication of this lattice for operation at these high frequencies continues to be extremely challenging.

New structures possessing full 3D photonic band gaps have been proposed which are easier to fabricate by conventional microfabrication techniques. Examples include the so-called 'woodpile structure' [29] [30] which can be made by micromachining [31], a square-spiral geometry PC [32][33] which can be fabricated using glancing angle deposition (GLAD) [34], and a tetragonal lattice of slanted pores [35] which can be generated by direct laser writing [36].

2.7 Conclusion

In this first chapter, the three types of photonic crystals had been studied. The one, two, and three dimensional photonic crystals are characterized by the number of directions that the dielectric periodicity exists with. In such way, this potential periodicity introduces a photonic band gap similar to this of the electron, where the photon is forbidden to propagate over it. This band gap, of the two dimensional PCs, gives the possibility to manipulate a new design of optical waveguide that will be studied in the next chapter.

Chapter 3

The photonic crystal fiber

3.1 Introduction

Photonic crystal fibers (PCFs) are one from the main important application of the 2D photonic crystal that is mentioned in the last chapter. They are fibers with an internal periodic structure made of capillaries, filled with air, laid to form a hexagonal, tetragonal, or any other lattice. Light can propagate along the fiber in defects of its crystal structure. A defect is realized by removing one or more central capillaries. PCFs are a new class of optical fibers.

Combining properties of optical fibers and photonic crystals they possess a series of unique properties impossible to achieve in classical fibers.

In this chapter we will take a general idea about this new design of optical fibers: the photonic crystal fiber (PCF) or the microstructure optical fiber, also it called the hollow fiber. We start with historical notes and the main developments that the PCF passed through. Then we show a description of the PCF geometry and the two guiding mechanisms that light travels with over the whole length. Later, we pass to the PCF proprieties such as the chromatic dispersion, the birefringence and the loss mechanisms. These characteristics will be discussed in details practically in the next chapters. Next, we see the interesting applications of this fiber where it can be used in both direct and indirect way. In the end of this chapter, we take a look about the two main methods of fabrication.

3.2 Presentation of PCF

3.2.1 Historical notes

As it is mentioned in the previous chapter, PBG originally predicted in 1987 by Sajeev John, from University of Toronto, and Eli Yablonovitch, from Bell Communications

Research, has become the really hot topic in optics in the early 1990s. The idea was to build the right structures, in order to selectively block the transmission of photons with energy levels that is wavelengths, corresponding to the PBGs, while allowing other wavelengths to pass freely.

Unfortunately, building the right structures has proved extremely difficult. The first PBG material was created in 1991 byYablonovitch and his colleagues by drilling holes with a diameter of 1mm in a block of material with a refractive index of 3.6. Since the bandgap wavelength is of the order of the spacing between the air-holes in the photonic crystal, this structure had a bandgap in the microwave region.

In 1991, Philip Russell, who was interested in Yablonovitch's research, got his big "crazy" idea for "something different," during CLEO/QELS conference [37]. Russell's idea was that light could be trapped inside a fiber hollow core by creating a two-dimensional photonic crystal in the cladding that is a periodic wavelength-scale lattice of microscopic air-holes in the glass.

The first fiber with a photonic crystal structure was reported by Russell and his colleagues in 1995 [38]. Even if it was a very interesting research development, the first PCF did not have a hollow core, as shown in figure 3.1, and, consequently, it did not rely on a photonic bandgap for optical confinement.

In fact, in 1995 Russell's group could produce fiber with the necessary air-hole triangular lattice, but the air-holes were too small to achieve a large air-filling fraction, which is fundamental to realize a PBG. Measurements have shown that this solid-core fiber formed a single-mode waveguide, that is only the fundamental mode was transmitted, over a wide wavelength range.

Moreover, the first PCF had very low intrinsic losses, due to the absence of doping elements in the core, and a silica core with an area about ten times larger than that of a conventional single-mode fiber (SMF), thus permitting a corresponding increase in optical power levels.

After moving his research group to the University of Bath in 1996, where PCF fabrication techniques were steadily refined, Russell and his co-workers were able to report, in 1999, the first single-mode hollow-core fiber, in which confinement was due by a full two-dimensional PBG, as reported in figure 3.2.

Today many laboratories throughout the world are interested in this type of fiber. They had made a big number of studies for almost a decade using the modeling methods to the exploitation of their novel properties [40]. Several commercial companies such as Blaze Photonics (Great Britain) [41] Crystal Fibers (Denmark) [42] and Redfern Polymer Optics (Australia) [43]...etc market these products.

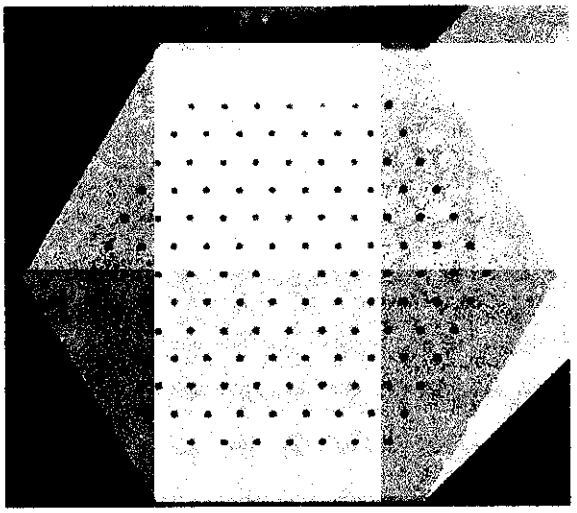

Figure 3.1: schematic of the cross-section of the first solid-core photonic crystal fiber, with air-hole diameter of 300 nm and hole-to-hole spacing of 2.3 μm, proposed in [38].

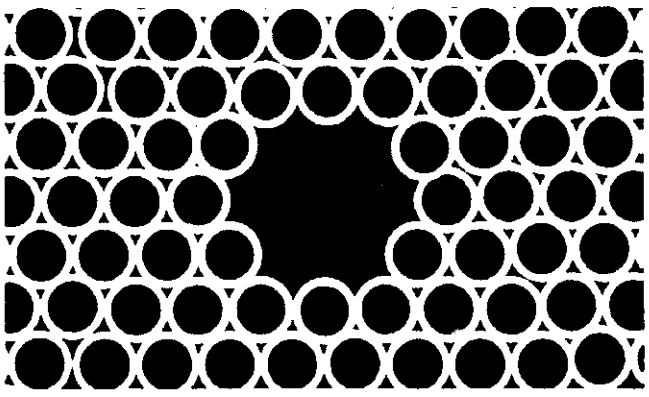

Figure 3.2: schematic of the cross-section of the first hollow-core PCF, with hole-to-hole spacing of 4.9 μm and core diameter of 14.8 μm, proposed in [39].

3.2.2 Geometry of PCF

The PCF is an optical fiber with a core surrounded by a cladding which consist an arrangement of air holes through the whole length of this fiber. The figure 3.3 shows the different parameters that define the optical proprieties of the PCF:

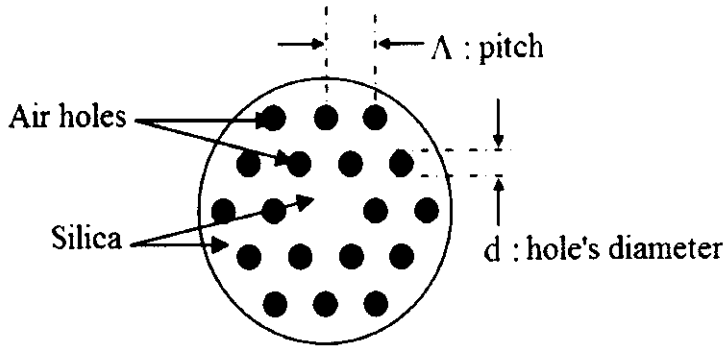

Figure 3.3: schematic representation of a cross-section of PCF structure, with solid core surrounded by 2 rings disposed in triangular lattice

The distance between the centers of two adjacent holes or the pitch and the hole diameter are the important criteria that characterize the PCF, those criteria can give the ratio d/Λ, which is the air fraction in the fiber. Also the number of rings of air holes that form the cladding is an important criterion, where it is used to reduce the loss resulting from light guiding or the confinement loss.

Compared with the conventional fiber, the PCFs can be characterized by their high design flexibility and the high refractive index contrast. The presence of the air holes in the cladding region reduces the effective refractive index of the cladding, that's confines light, more or less strongly, in the solid core. Depending on the arrangement of the air holes in the cladding region, it is possible to modify the propriety

The disposition of the air holes in the cladding region can be hexagonally, triangularly or randomly.

3.2.3 Guiding mechanism

Two types of guiding mechanism in the PCF can be distinguished all depending on the core nature. The hollow core PCF in which the guidance is over the photonic band gap (PBG) mechanism. In the solid core PCF, the guiding is happened following to the total internal reflection (TIR). This last is the one that we will work with in the whole project. Figure 3.4 shows an example for each kind of these types.

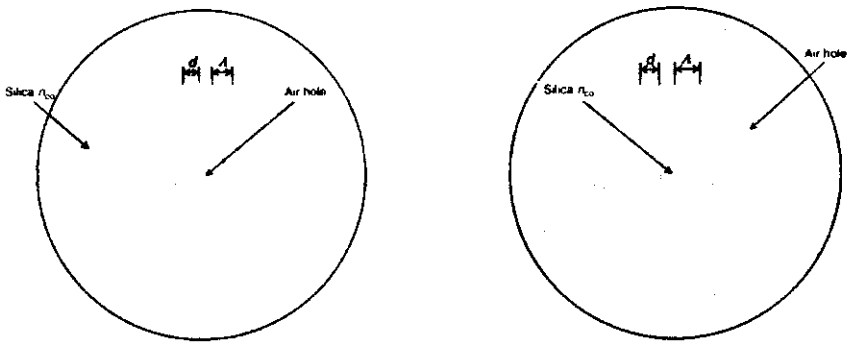

Figure 3.4: schematic cross section of a microstructured fiber with triangular lattice of air-holes. (a) Hollow core PCF. (b) Solid core PCF.

Modified total internal reflection

The PCF, also known as index-guiding PCFs, can be approximated to step-index optical fiber which guides the light with the classical form of total internal reflection. For deeper understanding, here is the principle of guiding mechanism in the standard fiber, which is also available with the PCFs:

$$kn_{core} < \beta < kn_{cladding} \tag{3.1}$$

With n_core and $n\_cladding$ are the refractive index of the core and cladding, respectively. k and β are the wave vector and propagation constant, respectively.

In order to form a guided mode in an optical fiber, it is necessary to introduce light into the core with a value of β, that is the component of the propagation constant along the fiber axis, which cannot propagate in the cladding. The highest β value that can exist in an infinite homogeneous medium with refractive index n is $\beta = nk_0$, being k_0 the free-space propagation constant. All the smaller values of β are allowed.

A two-dimensional photonic crystal, like any other material, is characterized by a maximum value of β which can propagate. At a particular wavelength, this corresponds to the fundamental mode of an infinite slab of the material, and this β value defines the effective refractive index of the material.

One can notes that this kind of guiding mechanism is called with "modified" TIR because there is not a clear interface defines the core and the cladding.

Photonic band gap guidance

Hollow Core Photonic Crystal Fiber (HCPCF) guides light by the Photonic Band Gap (PBG) effect. Light guiding is only possible if a photonic bandgap exists. Light guidance is then an analogue of a mechanism known in solid state physics as the electron conduction mechanism in materials with an energy-band structure. Periodically distributed air-holes can form a 2D photonic crystal structure with lattice constant similar to the wavelength of light. In 2D crystal structures photonic bandgaps exist which prevent propagation of light within a certain range of frequencies. If the periodicity of the structure is broken with a defect, a special region with different optical properties can be created. The defect region can support modes with frequencies falling inside the photonic bandgap, but since around this defect there is a photonic bandgap, light within the defect will remain confined in the vicinity of the defect. Modes falling outside the defect will be refracted, while modes falling inside the defect region will be strongly confined to the defect and guided along it throughout the entire length of the fiber [44].

Suppose a hollow-core PCF is designed to work in the red visible region of the electromagnetic spectrum. When the PCF is illuminated by a blue LED, all light will be refracted and no light will be guided by the fiber, consequently no light will come out at the end of the PCF. On the other hand, if the PCF is illuminated by a broadband source the red component of light will be guided appearing at the fiber end and all other frequency components of light will be refracted (figure 3.5).

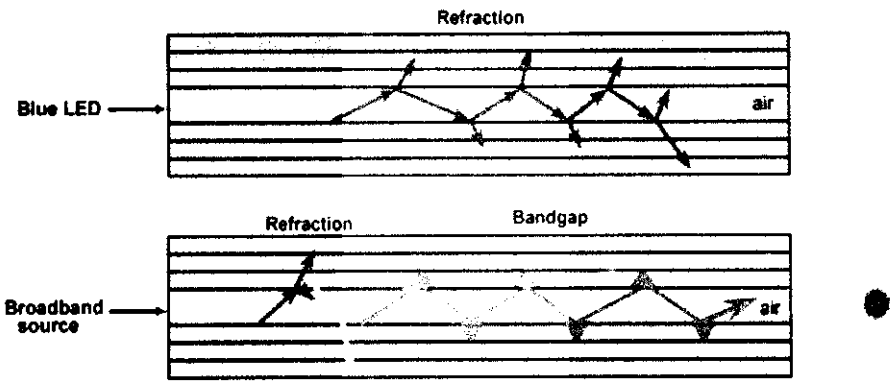

Figure 3.5: hollow-core PCF guidance of light through PBG

3.3 PCF proprieties

In this section, the optical characteristics of the photonic crystal fiber will be studied

3.3.1 Endlessly single modeness

There is an important proper propriety in the PCF which is the endlessly single mode, where the fiber can be single mode over a wide spectral range, regardless of the wavelength. So only the fundamental mode is guided. When the wavelength becomes shorter, the effective index of the cladding moves closer to the full silica (without air-holes). Indeed, as the effective index of the cladding becomes closer to the core's one, as the wavelength is short, and so the fiber rest single mode for all the wavelengths.

Russell has explained that the endlessly single-mode behavior can be understood by viewing the air-hole lattice as a "sieve" [45]. Since light is evanescent in air, the air-holes act like strong barriers, so they are the "wire mesh" of the sieve. The field of the fundamental mode is the "grain of rice" which cannot escape through the wire mesh, being the silica gaps between the air-holes belonging to the first ring around the core too narrow. On the contrary, the lobe dimensions for the higher-order modes are smaller, so they can slip between the gaps. When the ratio d/Λ increases, successive higher-order modes become trapped (figure 3.9). A proper geometry design of the fiber cross-section thus guarantees that only the fundamental mode is guided.

A numerical analysis says that the normalized effective frequency V_eff varies proportionally in a function of the ratio d/Λ.

$$V\_eff = \frac{2\pi a}{\lambda}\sqrt{n_{core}^2 - n_{eff}^2} \tag{3.2}$$

Where a is the radius of the PCF core. n_{core} and n_{eff} are the core refractive index and the effective refractive index of the PCF cladding, respectively.

Thus, the realizing of air holes with small diameter or large pitch is enough to maintain V_eff below 2.405 (cut off frequency of the fundamental mode in the standard fiber), and a guiding over single mode.

3.3.2 Chromatic Dispersion

When an optical pulse travels through an optical fiber, it will be affected by the dispersion; these phenomena can be explained by the temporal spreading of this pulse. The chromatic dispersion, or equivalently the group velocity dispersion, plays a fundamental role in conventional fiber optics, in the linear or in the nonlinear optical regimes, and this remains true when microstructured optical fibers are considered.

The chromatic dispersion D_c can be considered as the sum of the material dispersion D_M and the waveguide dispersionD_W.

$$D_c = D_M + D_W \tag{3.3}$$

The material dispersion is caused by the silica that composes the majority of the fiber, and that because of the dependence of refractive index of the silica on the wavelength, thus the dependence of the propagation velocity on frequency.

The waveguide dispersion can be defined as the dependence of the propagation constant on wavelength.

For a given propagation mode, the chromatic dispersion D_c is linked to the spectral evolution of the effective index n_{eff} by the following equation:

$$D_c = -\frac{\lambda}{c}\frac{d^2 n_{eff}}{d\lambda^2} \tag{3.4}$$

Where c is the speed of light in the vacuum. n_{eff} is the effective index ,this last depends on the indexes of the core and of the cladding, as well as on the distribution of the field over the two regions of the fiber. It was stressed quite early in the development of PCFs that these new waveguides could exhibit specific and interesting dispersion properties, and therefore that they might be considered for the management of chromatic dispersion in optical systems.

The control of the chromatic dispersion in PCFs is indeed much more powerful than in conventional optical fibers due to the higher index contrast and to the greater number of available geometrical parameters, for instance the diameters of the holes, the period of the lattice and more generally the location of the holes in the array.

3.3.3 Birefringence

The fundamental mode HE_{11} of the single-mode optical fiber is composed of two electromagnetic modes characterized by their perpendicular directions of polarization. In the case of ideal single-mode fiber, those two modes, denoted HE_{11x} and HE_{11y}, have the same propagation speed. In other case, when the optical fiber is birefringent due to structural defects, the symmetry in propagation constant between the two modes is broken and the difference between them becomes remarkable.

Both of modes HE_{11x} and HE_{11y} polarized in x and y directions (default polarization axes) have a different effectives indices n_{effx} and n_{effy}. Thus, the polarization status of the guided wave changes along the fiber. The birefringence between the two orthogonally axis can be expressed as:

$$B_\varphi = n_{effx} - n_{effy} \tag{3.5}$$

For an isotropic fiber, the polarization directions x and y are mentioned, also the effective indices n_{effx} and n_{effy} are identical. Therefore, the injected wave is conserved

along the propagation. Contrary, the cross section of an anisotropic fiber has only two perpendicular directions x and y, so only the injected wave within those directions conserves its polarization.

A wave linearly polarized within the axis, which has the low effective index (fast axis), has a group velocity higher than another polarized along the axis with a high effective index (slow axis). Those particular axes of the fiber are called the principal axes.

Polarization mode dispersion

The polarization mode dispersion (PMD) is defined as the difference of group delay per unit length:

$$PMD = \frac{(t_x - t_y)}{L} \tag{3.6}$$

The relation between the PMD and the group-mode birefringence depends on the coupling between the two polarizations.

In the short distance systems, where there is no coupling, the group delays are:

$$t_x = \frac{N_{gx}.L}{c} \tag{3.7}$$

$$t_y = \frac{N_{gy}.L}{c} \tag{3.8}$$

Where the relation between the PMD and the group-mode birefringence is:

$$PMD = \frac{B_g}{c} \tag{3.9}$$

One can observe that in the time domain, the propagated frequencies over the principal axes don't transmit at the same velocity and that because of the temporal spreading of the pulse. In the other side, in frequency domain, the propagation status of the wave is varied in a function of the wavelength.

3.3.4 Loss

The most important factor for any optical fiber technology is loss. Losses in conventional optical fibers have been reduced over the last 30 years, and a further improvement is unlikely to be reached. The minimum loss in fused silica, which is around 1550 nm, is slightly less than 0.2 dB/km. This limit is important, since it sets the amplifier spacing in long-haul communications systems, and thus is a major cost of those systems [46].

Intrinsic loss

The optical loss α_{dB}, measured in dB/km, of PCFs with a sufficiently reduced confinement loss, which will be described later, can be expressed as:

$$\alpha_{dB} = \frac{A}{\lambda^4} + B + \alpha_{OH} + \alpha_{IR} \tag{3.10}$$

Being A, B the Rayleigh scattering coefficient, the imperfection loss, respectively. α_{OH}, α_{IR} are OH and infrared absorption losses, respectively. At the present time the losses in PCFs are dominated by OH-absorption loss and imperfection loss [47].

In a typical PCF, the OH-absorption loss is more than 10 dB/km at 1380 nm and this causes an additional optical loss of 0.1 dB /km in the wavelength range around 1550 nm. Since this contribution is very similar to the intrinsic optical loss of 0.14 dB/km for pure silica glass at this wavelength, the OH-absorption loss reduction becomes an important and challenging problem. Most of the OH impurities seem to penetrate the PCF core region during the fabrication process. As a consequence, a dehydration process is useful in reducing the OH-absorption loss [47].

Imperfection loss, caused mainly by air-hole surface roughness, is another serious problem. In fact, during the fabrication process, the air-hole surfaces can be affected by small scratches and contamination. If this surface roughness is comparable with the considered wavelength, it can significantly increase the scattering loss. Thus, it is necessary to improve the polishing and etching process, in order to reduce the optical loss caused by this roughness. Moreover, fluctuation in the fiber diameter during the fiber drawing process can cause an additional imperfection loss, if the air-hole size and pitch change along the fiber [47].

It is important to underline that the Rayleigh scattering coefficient of PCFs is the same as that of a conventional SMF. However, this is higher than that of a pure silica-core fiber, although the PCF is made of pure silica glass. It is necessary to reduce the roughness further, in order to obtain a lower imperfection loss and a lower Rayleigh scattering coefficient [47].

Confinement loss

In both solid-core and hollow-core PCFs it is necessary to consider another contribution to the losses, that is the leakage or confinement losses. These are due to the finite number of air-holes which can be made in the fiber cross-section. As a consequence, all the PCF guided modes are leaky.

For example, in solid-core PCFs light is confined within a core region by the air-holes. Light will move away from the core if the confinement provided by the air-holes is inadequate. This means that it is important to design such aspects of the PCF

structure as air-hole diameter and hole-to-hole spacing, or pitch, in order to realize low-loss PCFs. In particular, the ratio between the air-hole diameter and the pitch must be designed to be large enough to confine light into the core. On the other hand, a large value of the ratio makes the PCF multimode. However, by properly designing the structure, the confinement loss of single-mode PCFs can be reduced to a negligible level.

It has been demonstrated a strong dependence of the confinement losses on the number of air-hole rings, especially for fibers with high air-filling fraction. In particular, leakage losses can be significantly reduced by increasing the rings number [48].

Bending loss

Conventional fibers suffer additional loss if bent more tightly than a certain critical radius. For wavelengths longer than a certain value, that is the "long-wavelength bend loss edge," all guidance is effectively lost. The same behavior is observed also in PCFs, which show even a "short-wavelength bend loss edge" [49], caused by bend-induced coupling from the fundamental to the higher-order modes, which leak out of the core. In fact, at short wavelengths the guided mode is mainly confined into the silica [49] and when $\lambda << \Lambda$, the field can escape through the interstitial space between the neighboring air-holes. As a consequence, the fiber becomes more sensitive to bending.

PCFs with larger relative air-hole diameters that are with higher d/Λ are less sensitive to bending loss. However, the demand for single-mode operation and the need for large-mode size limit the increase of d/Λ, and other solutions must be adopted. It has been demonstrated that the bending losses of triangular PCFs can be improved by changing the air-hole configuration from the traditional single-rod core design [50] [51]. In particular, an alternative structure with the core region formed by three silica rods has been proposed, with the aim to improve the guided-mode area and the resistance to the bending loss, particularly at the short wavelengths [50].

3.3.5 Effective area

All nonlinear effects are dependent upon the intensity of the electromagnetic field in the medium. However, it is the total optical power entering and leaving the fiber that is usually measured. The measured optical power leaving a fiber is simply the integral of the intensity distribution over the entire fiber cross section.

For a uniform intensity distribution I , over a core of area A_{core}, the intensity could be calculated from the measured power, P_{meas}, using:

$$I = \frac{P_{meas}}{A_{core}} \tag{3.11}$$

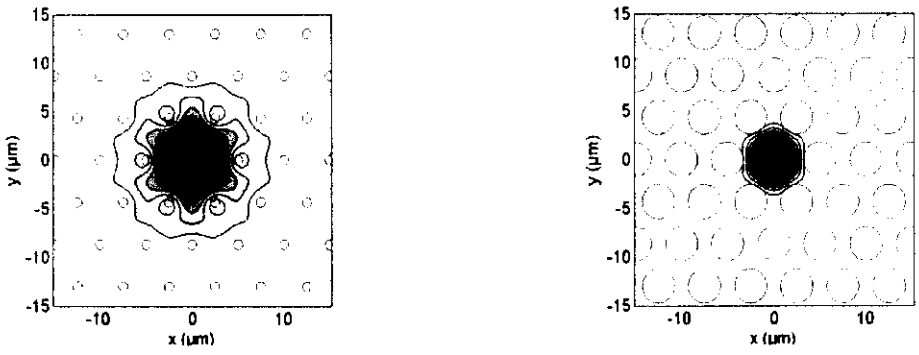

Figure 3.6: (a) PCF with large modal effective area (Λ=0.5μm; d/Λ=0.2). (b) PCF with small modal effective area (Λ=0.5μm; d/Λ=0.7)

However, the field in a single mode fiber is not evenly distributed or even fully contained within the core. It is larger at the fiber axis than near the core-cladding interface and extends into the cladding to a degree depending on the actual refractive index profile. Calculating a uniform intensity in the core using equation 2-1 will underestimate the value on the axis of the fiber and overestimate the value near the core-cladding interface.

The effective area parameter has been defined for the purposes of calculating non-linear effects [52]. It is a single value, based on the modal field distribution, and can be used in equation 2-1 instead of A_{core} to calculate a value for the optical intensity.

The effective area can be expressed as[53]:

$$A_{eff} = \frac{\left(\iint_{-\infty}^{\infty} \left|\vec{E}(x,y)\right|^2 dxdy\right)^2}{\iint_{-\infty}^{\infty} \left|\vec{E}(x,y)\right|^4 dxdy} \tag{3.12}$$

Where $\vec{E}(x,y)$ is the electrical field. The effective area is adjustable grace to the geometrical parameter: high Λ(Λ>0.5μm) or/and low d/Λ(d/Λ<0.3) [54]. Fig 2.5 shows the modal effective area of two PCFs with different opt-geometrical parameters.

Generally, the relation between the effective area and the geometrical parameters can be defined as [55]:

$$A_{eff} \propto \left(\frac{\Lambda}{d}\right)\Lambda^2 \tag{3.13}$$

The fiber with small modal effective area can be used as a no linear basic components, where the fiber with large modal effective area can used in the high power transmission.

3.4 Potential applications

The unusually proprieties of the photonic crystal fibers make it very attractive for a wide range of applications. Even though PCFs have been around for couple of years, the huge range of possible applications is far from being fully explored [56]. It is expected that this field will stay very lively for many years and give a lot of opportunities for further creative work, both concerning fiber designs and applications [56][57].

3.4.1 Direct applications

The direct applications mean the directly using of PCF with its intrinsic properties without making any modifications [58]:

Dispersion controller

The study of the chromatic dispersion in the PCF improves the possibility of using this propriety in the telecommunication domain. The flexibility of fabrication allows the PCF with zero dispersion threw large spectral range to be manufactured. Two ways can be used to control the dispersion, one by changing the geometrical parameters of the basic PCF, and the other by adapting the index profile.

Adjusting the geometrical parameters

The chromatic dispersion can be controlled by the main parameters of the PCF structure. Choosing the adequate diameter "d" and the hole to hole space "Λ" gives the advantage to get a very low or zero value of dispersion. A microstructured optical fiber with zero or very low dispersion at the 1.55 μm wavelength can be obtained with $\Lambda = 1.1\mu$m and d/ Λ=0.9 [59]. For a PCF with air hole's diameter of 0.316 μm and Λ= 2.62μm and a cladding with 7 rings, the dispersion is ultraplate ($D = 0 \pm 0.4ps/nm/km$) for large range (1230 to1720nm) [62]. Practically, Reeves et al [63] had fabricated a PCF with 7 rings and air holes of diameter 0.57μm spaced by 2.47μm where the measured chromatic dispersion is $0 \pm 1.2ps/nm/km$ between 1000 and 1600nm.

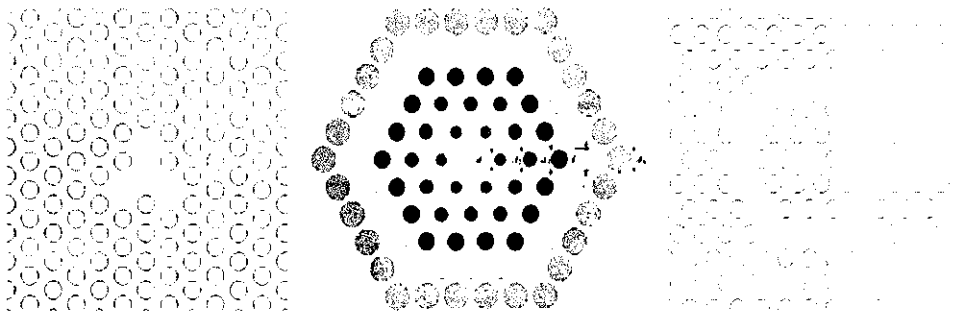

Figure 3.7: examples for index profiles using in dispersion controller

Adapting the index profile

During fabrication, it is hard to get a microstructured fiber which act as a dispersion controller with the desired parameters. Therefore, new configurations of the index profile have been used as showed in figure 3.7.

The first structure (a) is multi-core fiber which has a hybrid triple core surrounded with air/silica microstructured cladding arranged in a triangular lattice. The hybrid core consists a central region doped germanium (n=1.487) inclosed with three regions doped fluor (n=1.440), this regions have diameter equal to the pitch Λ. This fiber has a zero wavelength dispersion (ZWD) equal to 1.55 μm with d/Λ between 0.44 and 0.56, and a pitch varies between 1.24μm and 1.61μm.

The second structure (b) had been designed by Saitoh et al. and allows to get a flattened dispersion [60]. It is characterized by a different air holes diameter in every ring (the diameter d_i for the ring i). For a PCF with 4 rings and Λ=1.56μm, d_1/Λ=0.32, d_2/Λ=0.45, d_3/Λ=0.67 and d_4/Λ=0.95, the dispersion is $0\pm0.5ps/nm/km$ between 1.19μm and 1.69μm. In the other side, a PCF with 5 rings and Λ=1.58μm, d_1/Λ=0.31, d_2/Λ=0.45, d_3/Λ=0.55, d_4/Λ=0.63 and d_5/Λ=0.95 , has a chromatic dispersion of $0 \pm 0.4ps/nm/km$ between 1.23μm and 1.72μm.

The third PCF is a dual-core fiber, and it used for the compensation of the negative dispersion of -19000ps/nm/km at 1.55μm and effective area of 30μm^2 [61]. It is formed by the absence of the 3rd ring from a normal solid core PCF.

The third PCF is a dual-core fiber, and it used for the compensation of the negative dispersion of -19000ps/nm/km at 1.55μm and effective area of 30μm^2 [61]. It is formed by the absence of the 3rd ring from a normal solid core PCF.

Polarization controller

In order to achieve a birefringent fiber, spatial asymmetry in the index profile can be used, also by applying asymmetrical stress to the core region. Breaking the symmetry of the fiber will lead to a new type of PCF, which allows controlling the polarization of light. This last is so useful in the telecommunication domain. Changing the holes' diameter or their arrangement in the cladding region makes the light propagate in different velocities depending to their polarization status. Actually, the birefringence obtained by the PCF is more important of this in the conventional fiber (10 times higher). Some birefringent PCFs allow compensating the different in light polarization status that's travels for long distances, using only a short length of this fiber (HI-BI PCF).

3.4.2 Indirect applications

This type of applications includes the components and the systems based on the PCF:

Laser

An interesting application of photonic crystal fiber (PCF) technology concerns the realization of efficient high power fiber lasers by means of endlessly single mode PCFs with very large mode areas (LMAs). The implementation of air-clad LMA-PCF lasers [64] is particularly advantageous because it leads to a very high numerical aperture for the inner cladding, providing efficient pump launching, reduced pump threshold and high pump absorption. Traditional active fibers, like those used for telecommunication amplifiers, are basically standard transmission fibers where the core region has been doped with rare-earth ions. This fiber type is pumped with single-mode pump lasers and is known as core-pumped fibers. The power limitations of single-mode pump sources make these types of fibers unsuitable for high power applications (on the order of 1W and upwards). High power fibers are commonly designed with a double-cladding structure, where a second low index region acts as cladding for a large pump core. In the center of the pump core is located a much smaller doped signal core (see figure 3.8). The major advantage of the double cladding design, over the more traditional core pumped variety, is the large pump area and high numerical aperture, enabling pumping with relatively low-cost multimode diodes and diode bars/stacks [65].

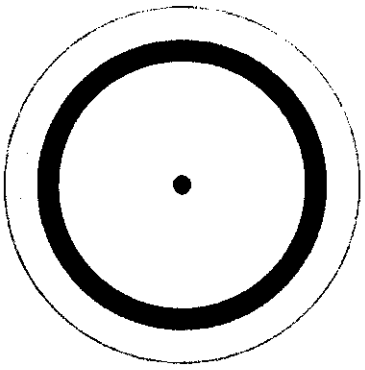

Figure 3.8: cross section of a standard step-index double-clad fiber with an active single-mode core (black) surrounded by a large multimode pump guided (light gray). The pump guide is coated with a low index polymer cladding (dark gray)

Sensor

Optical fibers based sensors are low cost and efficient solutions for several industries due to their high sensitivity, small size, robustness, flexibility and ability for remote monitoring as well as multiplexing. Other advantages entail their aptitude to be used even in the presence of unfavorable environmental conditions such as noise, strong electromagnetic fields, high voltages, nuclear radiation, in explosive or chemically corrosive media, at high temperatures, among others. For example curvature sensing has been demonstrated with multi-core fiber [66]. When the fiber is bend, the phase difference between the two cores changes, which can be detected from the output spectrum. Sensors for gases or liquids (for example detecting the concentration of pollutants in a gas) have also been explored [67].

Long Period Grating

Long period gratings (LPGs) consist of a large scale (hundred's of microns) periodic axial perturbation in the core of a single-mode optical fibre [68]. The effect of an LPG is to couple light of certain well-defined wavelengths from the core of the fibre to various cladding modes; the coupled light is then lost from the fibre, leading to a series of attenuation bands in the transmission spectrum of the device. From a sensing perspective, LPGs are of interest as the positions of the attenuation bands are sensitive to a number of measurands: temperature, strain, external refractive index and curvature.

A feature of LPGs is that the sensitivity to the various measurands is strongly de-

pendent on the dispersion properties of the core and cladding [68]; consequently control of the material or waveguide dispersion can, in principle, be used to increase sensitivity to one measurand while rendering the device insensitive to another. Photonic crystal fiber (PCF) might offer great potential in this regard since the waveguiding properties can be controlled simply by adjusting the air-hole geometry. Recently, it has been shown that LPGs can be produced in non-photosensitive PCF by periodically collapsing the holes by heat treatment with a CO2 laser [69] or by using an electric arc to modify the fiber structure [70]. In this paper we report the first experimental characterisation of the sensitivity of an electric arc-induced LPG in PCF to temperature, bending and strain.

PCF with filters

As described above, photonic crystal fibers can be used for laser generation and sensing, but they can also include filtering functions. Photonic crystal fibers can be used as optical filters. A short-wavelength filter, which consists of a photonic crystal fiber with a depressed-index core but guides with total internal reflection, was fabricated [71]. The effective index of the cladding increases for decreasing wavelengths and finally exceeds that of the core.

Light with wavelength shorter than that wavelength is not guided in the fiber. Optical filters and attenuators can also be realized by incorporating a doped region in the core allowing for grating writing and/or infusing cladding air-holes with active materials yielding tunable devices. Band rejection filters for flattening the gain of optical amplifiers were demonstrated using a long period grating written in the core. The grating induced coupling between the mode in the core and co-propagating cladding mode(s) due to phase matching which results in resonant loss at a certain wavelength [72]. The filters can be made tunable when active material is infused in the air holes. The cladding mode frequency is strongly affected when the refractive index of the active material is changed which affects the wavelength of the resonant loss [72]. Tunability can be achieved with, for example, temperature or electric field depending on the active material

3.5 Fabrication process of PCF

One of the most important aspects in designing and developing new fibers is their fabrication process. The PCF is made up with pure fused silica and an arrangement of air-holes in the cladding region. This has several advantages, since air is mechanically and thermally compatible with most materials, it is transparent over a broad spectral

range, and it has a very low refractive index at optical frequencies. Also the silica is an excellent material to work with, because viscosity does not change much with temperature and it is relatively cheap.

3.5.1 Stack-and-draw technique

In order to fabricate a PCF, it is necessary, first, to create a preform, which contains the structure of interest, but on a macroscopic scale. However, a relatively simple method, called stack-and-draw, introduced by Birks et al. in 1996 [73], has become the preferred fabrication technique in the last years, since it allows relatively fast, clean, low cost, and flexible preform manufacture.

The PCF preform is realized by stacking by hand a number of capillary silica tubes and rods to form the desired air–silica structure, as showed in Fig 2.8. This way of realizing the preform allows a high level of design flexibility, since the core size and shape, as well as the index profile throughout the cladding region can be controlled.

After the stacking process, the capillaries and rods are held together by thin wires and fused together during an intermediate drawing process, where the preform is drawn into preform canes. This intermediate step is important in order to provide numerous preform canes for the development and optimization of the later drawing of the PCFs to their final dimensions [74]. Then, the preform is drawn down on a drawing tower, greatly extending its length, while reducing its cross-section, from a diameter of 20 mm to an 80–200 μm one. In order to carefully control the air-hole size during the drawing process, it is useful to apply to the inside of the preform a slight overpressure relative to the surroundings, and to properly adjust the drawing speed [74]. In summary, time dynamics, temperature, and pressure variations are all significant parameters which should be accurately controlled during the PCF fabrication. Finally, the PCFs are coated to provide a protective standard jacket, which allows the robust handling of the fibers. The final PCFs are comparable to standard fibers in both robustness and physical dimensions, and can be both striped and cleaved using standard tools.

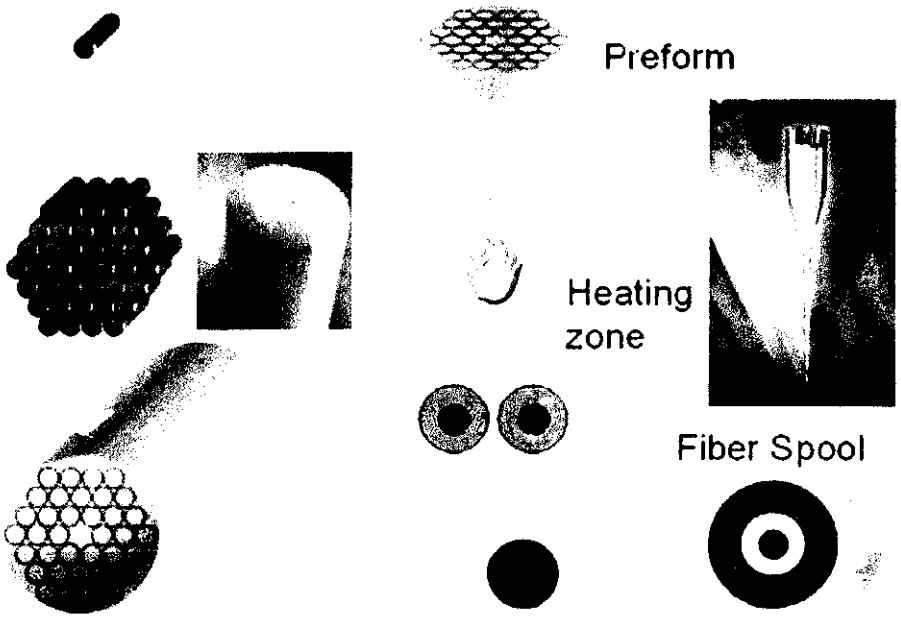

Figure 3.9: scheme of the Stack-and-draw technique for PCF fabrication process

3.5.2 Extrusion fabrication process

Extrusion is an alternative fabrication technology for PCF preforms [75], and this has recently been extended to the use of soft glasses [76]. Those last offer a range of useful properties not possessed by silica, such as high refractive index, good infrared transmittance, high optical nonlinearity and relatively low phonon energy among oxide glasses [77]. In this fabrication process a molten glass is forced through a die containing a suitably designed pattern of holes. Extrusion allows fiber to be drawn directly from bulk glass, using a fiber-drawing tower, and almost any structure, crystalline or amorphous, can be produced. It works for many materials, including chalcogenides, polymers, and compound glasses. However, selective doping of specified regions, in order to introduce rare earth ions or render the glass photosensitive, is much more difficult.

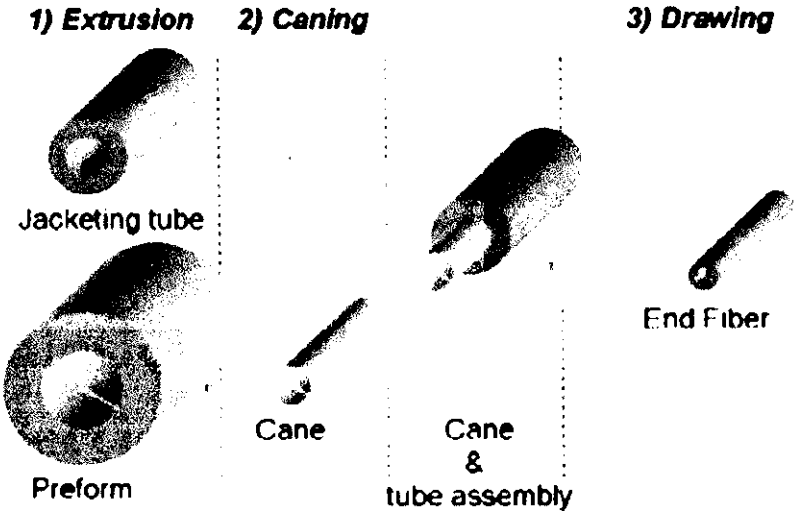

Figure 3.10: scheme of the extrusion technique for PCF fabrication process

3.6 Conclusion

At the end of this chapter, it is worth noting the impressive properties of this new design of optical fibers; the photonic crystal fiber has covered the "majority" of "few" weakness points of the conventional fiber. The fully pure silica structure has minimized the attenuation caused by the impurities. In addition, the refractive index contrast between the core and the cladding is applied by the air holes existing in the cladding region. This design also gives the possibility to be mono-modeness over wide range of wavelengths. The tailorable dispersion propriety was the solution for an obsession problem; so it can be shifted zero dispersion, flattened dispersion or highly negative dispersion at any operation wavelength. The high degree of flexibility, and also of fabrication process, gives rise to many practical applications in optical communications, nonlinear optics, various optical devices and sensors.

Chapter 4

Simulation of the optical properties of PCF

4.1 Introduction

In the last chapter, the proprieties of the photonic crystal had been studied theoretically. These proprieties will be discussed practically in this chapter. In order to investigate the endlessly single modeness, the chromatic dispersion, the confinement loss, and the birefringence, the photonic crystal fiber will be simulated and characterized with the commercial software OptiFDTD® from Optiwave Corporation, based on the finite difference time domain method (FDTD) which is one of the most powerful techniques to investigate linear and nonlinear light wave propagation phenomena in axially varying waveguides which is also quite useful for the light pulse propagation in optical fibers.

4.2 Endlessly single modeness

One of the attractive properties of the PCFs is their possibility to be single-moded over a wide wavelength range, surpassing the ordinary single-mode fibers which become multi-moded for wavelength below their single-mode cut-off wavelength. PCFs, which are specially designed with this property, are called endlessly single-mode (ESM) PCFs [78].

A simple model used to study the PCF is effective index model, where the high index core surrounded by the lower effective index of the cladding due to the presence of the periodic holes. In the case of cladding with small air-filling-fraction, one will get a low index-contrast equivalent waveguide, which is required for single-mode operation.

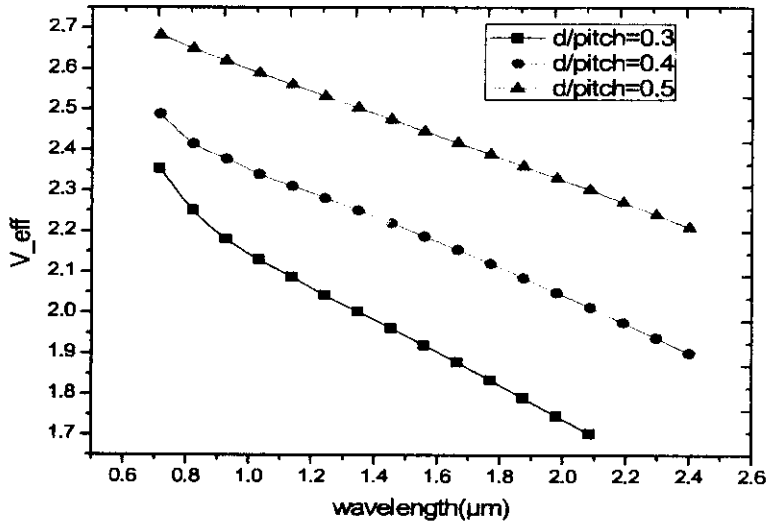

Figure 4.1: variation of effective frequency with wavelength for different diameters of air holes

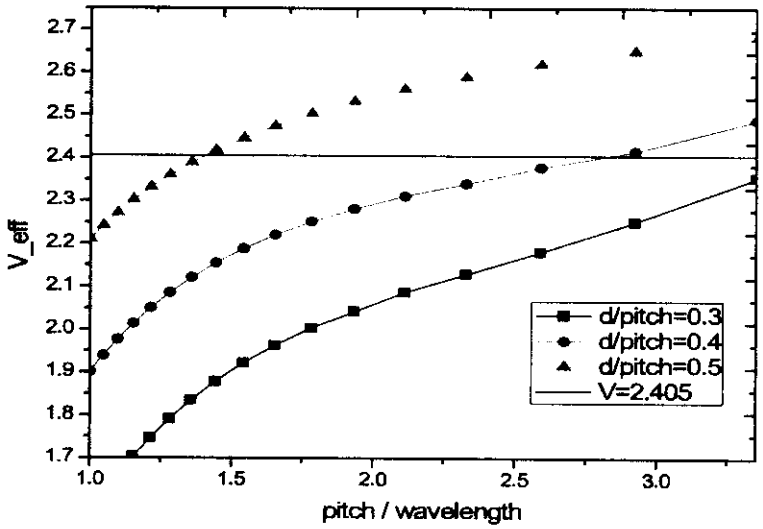

Figure 4.2: variation of effective frequency Veff with normalized frequency a/λ for various relative hole diameters. The dashed line indicates Veff = 2.405.

At shorter wavelengths, the effective index of the cladding will get closer to the refractive index of the silica. This dispersive property will somehow compensate the decrease of the wavelength and keep the single-mode behavior over a wide wavelength range.

This is fundamentally different from the conventional fibers where, at huge core diameter to wavelength ratios, a multi-mode operation is unavoidable at shorter wavelengths, because the cladding index is constant and normalized frequency arises with wavelength, once exceeding the value critical for single-mode operation. In addition, the presence of air holes in the cladding can change the spectral characteristics of microstructured fibers.

Theory indicates that PCFs are single-mode over a wide range of wavelengths or pitch sizes as long as $d/\Lambda<0.45$ [78]. PCFs with a ratio $d/\Lambda>0.45$ can carry higher order modes.

Using equation 3.2, we calculated the Veff parameter for different air filling ratios for a PCF with 5 rings arranged in triangular lattice. It is observed from figure 4.1 and figure 4.2 that the Veff parameter decreases with an increase of wavelength and increases with an increase in normalized frequency.

It is clearly observed from the figure 4.2 that the PCF with air fraction of 0.3 is completely single mode over the whole used range and nearly to be with air fraction of 0.4, while it is multimode with 0.5. This proves the theory discussed before.

4.3 Confinement loss

This loss is due to the leaky modes which are generated when the core is surrounded by a few numbers of rings of inclusions. Its factor can be calculated by using this formula:

$$L = 8.686 k_0 Im[n_{eff}] \tag{4.1}$$

In decibels per meter, $Im[n_{eff}]$ is the imaginary part of the effective index.

In order to better explain the leakage loss behavior in PCFs, a solid-core fiber surrounded with five rings arranged in both triangular and rectangular lattice of air-holes is here considered. This fiber has a fixed pitch $\Lambda = 3$ μm and different diameter of air holes varying between 0.8 μm and 2.8 μm.

The refractive index of silica is computed by using the Sellmeier equation:

$$n_{silica} = [1 + \frac{0.6961663\lambda^2}{\lambda^2 - (0.0684043)^2} + \frac{0.4079426\lambda^2}{\lambda^2 - (0.1162414)^2} + \frac{0.8974794\lambda^2}{\lambda^2 - (9.896161)^2}]^{1/2} \tag{4.2}$$

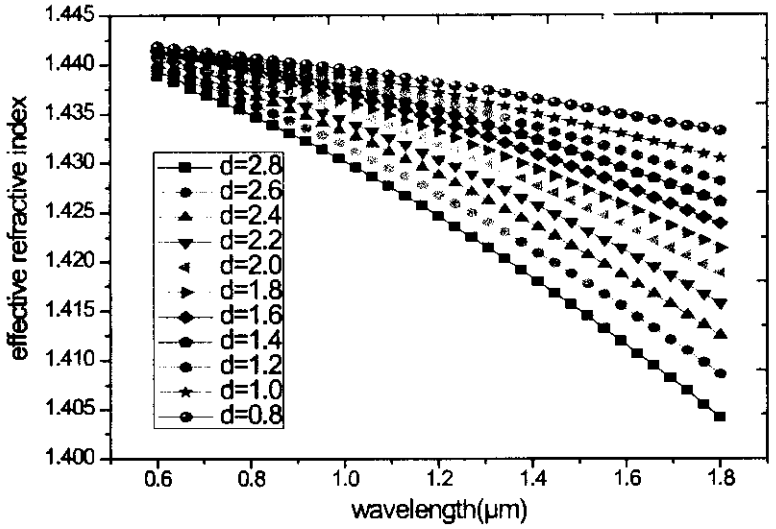

Figure 4.3: evolution of the effective refractive index with wavelength for different diameters of air holes

Over the last figures (figure 4.4 and figure 4.5), it can be seen the powerful effect of the air holes in the guiding operation. Figure 4.4(b) shows the concentration of the optical field intensity into the solid core, while it is distributed over a large area in the figure 4.4 (b). This is because of the size of the air holes. The big size of air holes as shown in figure (a) helps to confine light into the core and thus reducing the confinement loss, contrary in the case where the small size air hole is used (figure (b)).

Generally, the difference between the two structures is in the confined field form, so it is hexagonal with the triangular lattice and square by using the tetragonal lattice.

At the shorter wavelength the light will be more confined in the core part hence the confinement loss will be low and loss will increase as wavelength increases.

Figure 3.3 shows the variation of the confinement loss with wavelength. It is observed that leakage loss becomes less with high values of air holes diameter and so high air fraction (d/Λ). It is nearly zero up to 1 μm for all the tested holes sizes, and keeps so for the big sizes one (higher than 1.4μm) with the higher wavelengths, while it is strongly increased for the rest.

(a) (b)

Figure 4.4: the distribution of field intensity for a PCF with triangular lattice at 1.55 μm wavelength (a) with air hole diameters of 0.8 μm. (b) with air holes diameter of 2.8 μm

(a) (b)

Figure 4.5: the distribution of field intensity for a PCF with tetragonal lattice at 1.55 μm wavelength: (a) with air hole diameters of 0.8 μm. (b) with air holes diameter of 2.8 μm

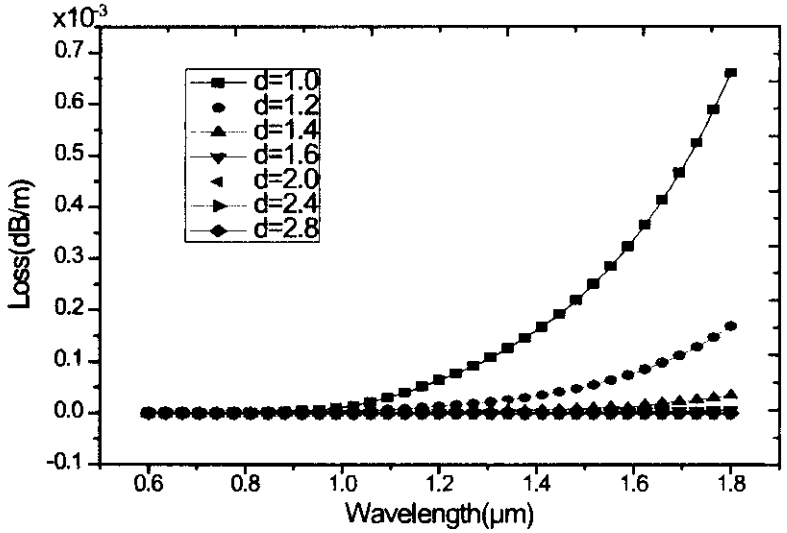

Figure 4.6: the evolution of confinement loss with wavelength for a triangular lattice PCF with fixed pitch $\Lambda = 3$ μm and different air hole diameters

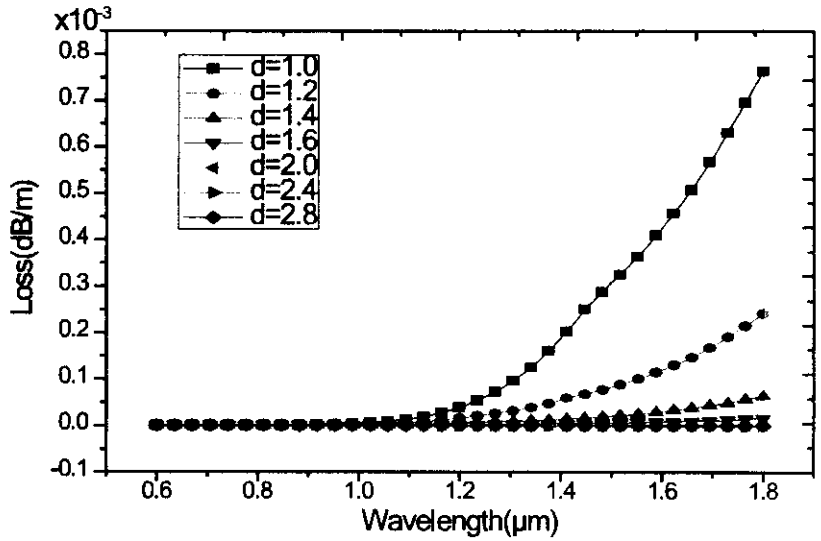

Figure 4.7: the evolution of confinement loss with wavelength for a tetragonal lattice PCF with fixed pitch $\Lambda = 3$ μm and different air hole diameters

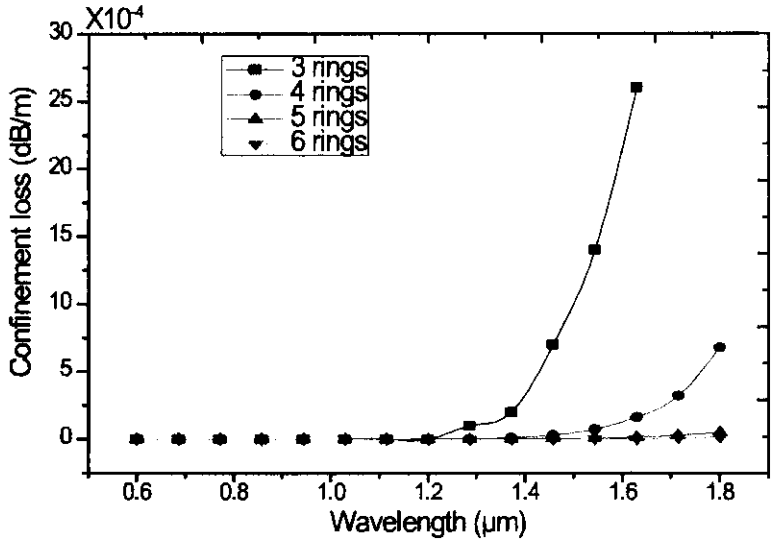

Figure 4.8: the evolution of confinement loss with wavelength for a tetragonal lattice PCF with fixed pitch $\Lambda = 3$ μm and different air hole diameters

The same observations here with the PCF with tetragonal lattice unless small difference in loss values.

As a first step, we had varied the diameter of the air holes to see their affection on the confinement loss. As a second step of this section, we will see the variation of leakage loss as function of wavelength for different number of rings that surrounded the solid core.

The structure used in this part of simulation has a fixed diameter of air holes (d=0.7 μm) and pitch ($\Lambda = 5$ μm). The refractive index of silica is also calculated by Sellmeier equation. A different number of air holes are used (3, 4, 5 and 6 rings).

It is known that the confinement loss in a PCF decreases rapidly as more rings of air holes are introduced in the cladding. The evolution of loss as shown in fig 3.4 improved that. However, the four structures have a nil loss up to 1.2 μm, and then it increases strongly in the case where 3 rings are used. This loss is less strongly in the case of 4 rings, while it keeps varying around zero for the rest PCFs (5 and 6 rings).

Since the air holes are more presented in the cladding region, therefore the air fraction is higher and so the contrast between the core and the cladding, thus the light is more confined.

4.4 Chromatic dispersion

Compared with conventional optical fibers, PCFs have shown their advantages in the control of chromatic dispersion which is very important for practical applications to optical communication systems, dispersion compensation, and nonlinear optics.

Up to now, control techniques of the chromatic dispersion of PCFs are very attractive, and various PCFs with specific dispersion properties such as dispersion flattened (DF) PCFs [79][80] and large negative dispersion PCFs [81][82] have been reported.

The dispersion discussed here is the chromatic dispersion (including the waveguide dispersion and the material dispersion), which can be calculated by 3.4 mentioned in the last chapter.

The aim of this section is to identify the behavior of chromic dispersion in function of wavelength using different air fractions.

Two structures of PCF are proposed here depending on the arrangement of air holes in the cladding region (tetragonal and triangular). The geometrical parameters of both structures will be characterized by a fixed pitch $\Lambda = 3\ \mu$m and variable diameter of the air holes. The material refractive index is computed by Sellmeier equation. The wavelength range that used in the simulation is between 0.6 and 1.8 μm choosing 35 iterations.

Both figures above (Fig 3.4 and Fig 3.5) show the simulation result of chromatic dispersion for both tetragonal and triangular lattice respectively. However, the chromatic dispersion increases with wavelength whatever the air fraction used. It starts with negative values (-350 ps/nm.km around 0.6 μm) and then it passes over the zero line and it becomes more and more stable with higher wavelengths.

It can be clearly seen the effects of the air fraction: when the diameter of air holes decreases and thus the air fraction ratio, the chromatic dispersion becomes low and more flattened. Also it can observed that the zero chromatic dispersion is shifted to the 1.55 μm wavelength (which is the operation wavelength used in telecommunications) every time the lower diameters are used.

Practically, both structures have nearly the same evolution of chromatic dispersion.

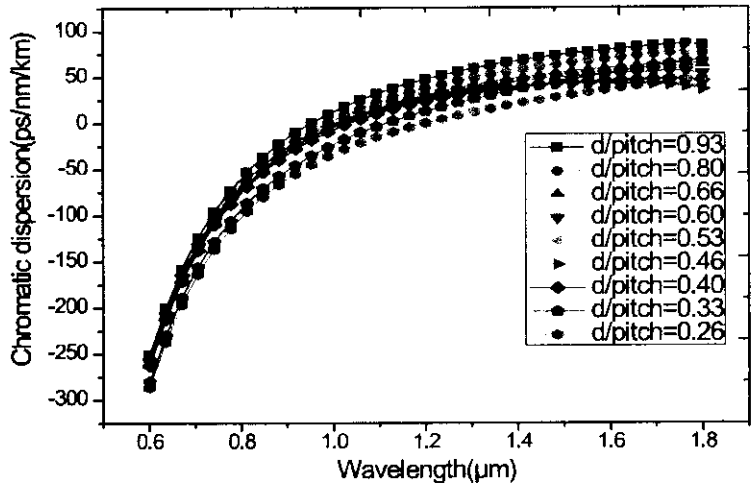

Figure 4.9: the variation of chromatic dispersion with wavelength for a tetragonal lattice PCF with fixed pitch $\Lambda = 3$ μm and different air hole diameters

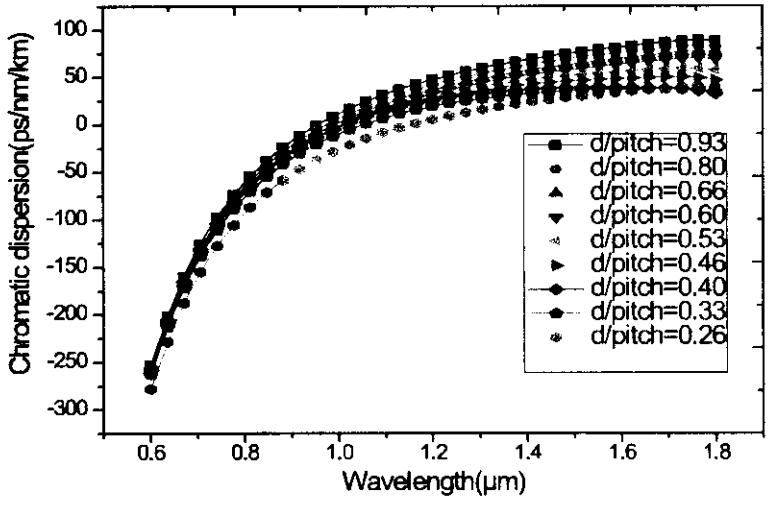

Figure 4.10: the variation of chromatic dispersion with wavelength for a triangular lattice PCF with fixed pitch $\Lambda = 3$ μm and different air hole diameters

4.5 Birefringence

As discussed in the previous chapter, the so-called single-mode fibers in fact support two modes simultaneously, which are orthogonally polarized. In an ideal circular-core fiber, these two modes will propagate with the same phase velocity; however, practical fibers are not perfectly circularly symmetric. As a result, the two modes propagate with slightly different phase and group velocities. Furthermore, environmental factors such as bend, twist, and anisotropic stress also produce birefringence in the fiber, the direction and magnitude of which keep changing with time due to changes in the ambient conditions such as temperature. These factors also couple energy from one mode to the other mode of the fiber, creating problems in practical applications. In this section, a numerical analysis will be reported with the aim to give an idea about the birefringence behavior for the two structures used before, PCF with triangular and tetragonal lattice, with different diameters of air-holes.

The two figures above (figure 4.11 and figure 4.12) show the evolution of birefringence versus wavelength for different air holes. Comparing between the two structures, the PCF with tetragonal lattice has higher birefringence than the PCF with triangular lattice especially when the big diameters are used. Practically, the birefringence doesn't depend on the size of air holes, as much as it on the difference between the two orthogonally axes that light propagates through, according to the 3.5.

However, this propriety will be extensively discussed in the next chapter with aim to study one from the wide used applications, the highly birefringence PCF.

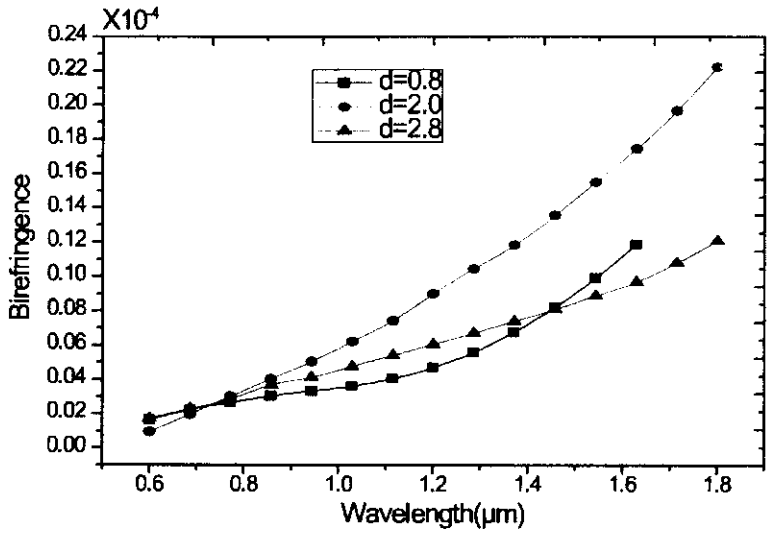

Figure 4.11: the variation of birefringence with wavelength for a tetragonal lattice PCF with fixed pitch $\Lambda = 3$ μm and different diameters of the air holes

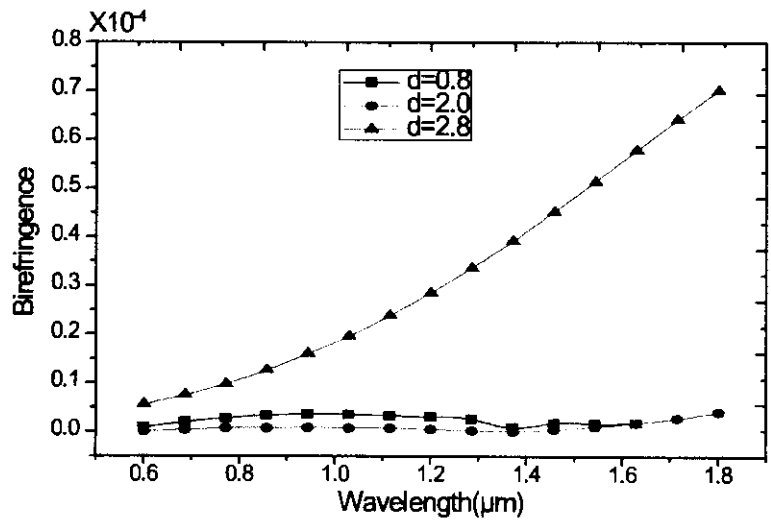

Figure 4.12: the variation of birefringence with wavelength for a triangular lattice PCF with fixed pitch $\Lambda = 3$ μm and different diameters of the air holes

4.6 Conclusion

In this chapter, the optical proprieties of the photonic crystal fiber had investigated practically. The endlessly monomodeness had been proved and it can be assured by using the air fraction ratios less than 0.4. Changing the air filling ratio causes the change in the confinement loss of the PCF. As the size of the air holes and so the number of rings in the cladding part of PCF increases the modes tends to be more confined in the core part and hence the confinement loss reduces. Hence confinement loss can be controlled by varying the air hole size in the cladding part of photonic crystal fiber. The behavior of chromatic dispersion indicates that since the air holes with smaller diameters are used, the chromatic dispersion tends to be more flattened. Also the variation of these diameters can shift the zero value dispersion to any desired wavelength. For the birefringence, it depends on the holey structure of the cladding rather than the size of the air holes, and generally it is low in the order of magnitude of 10^{-4}.

Chapter 5

Application: HI-BI photonic crystal fiber

5.1 Introduction

High birefringence (Hi-Bi) can be easily obtained with PCF because of the design flexibility and the high index contrast [88][89], giving the possibility to reach an order of magnitude of 10^{-3} or 10^{-2}, which is larger than conventional fibers (10^{-4}) [90]. Several approaches have been explored to achieve high birefringence in photonic crystal fibers. One can use elliptical instead of circular air-holes in the cladding region [91][93], another can employ air-holes with different diameters [94][96]. Filling selectively some air-holes by a liquid with a refractive index lower than silica is also investigated [97] [99].

In this chapter, we report the numerical analysis of several Hi-Bi PCF patterns with the aim to give an optimal design for the tradeoff between three criterions: the chromatic dispersion, the birefringence and the confinement loss. The analysis will be carried out using the Finite-Difference-Time-domain (FDTD) method. The investigated patterns are: The Pseudo-Panda PCF [90], the V type PCF [98] and the selectively liquid filled PCF [97] with the triangular and the tetragonal lattice. Based on three criterions:, the results will be analyzed and discussed.

5.2 Structures

Figure 5.1 shows the two main structures of our study. The index of silica is 1.46. Both structures are specified by two parameters, the radius of the air-holes and the pitch between two adjacent holes. Initially, the holes radius and the pitch are set to be

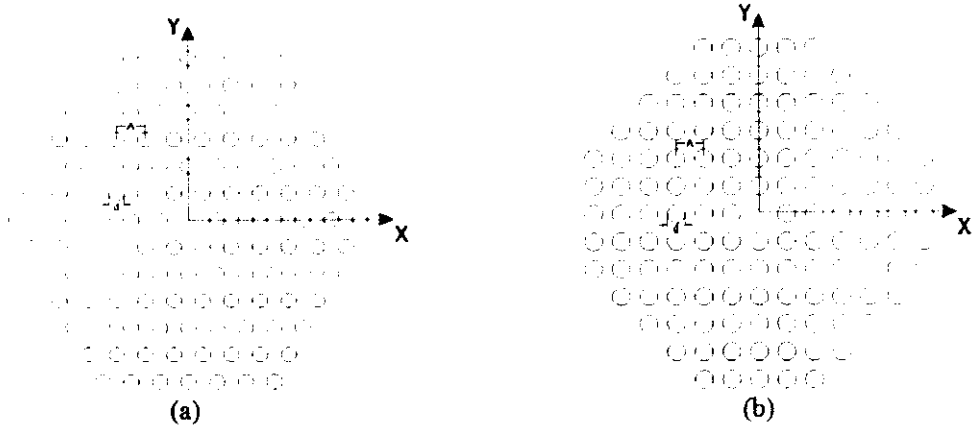

Figure 5.1: cross section of PCF with triangular lattice (a) and tetragonal lattice (b) with: d the holes radius and the pitch Λ

0.8μm and 2.3μm, respectively. To ensure that light is well confined in the structure, the cladding is selected to be formed by six layers (rings) of air-holes.

5.3 V type PCF

This kind of PCF was proposed by J. Wojcik et al for hydrostatic pressure sensing [98]. As it is shown in figure 5.2, the cladding is designed in such way to have selectively and differently sized holes in the form of the letter V.

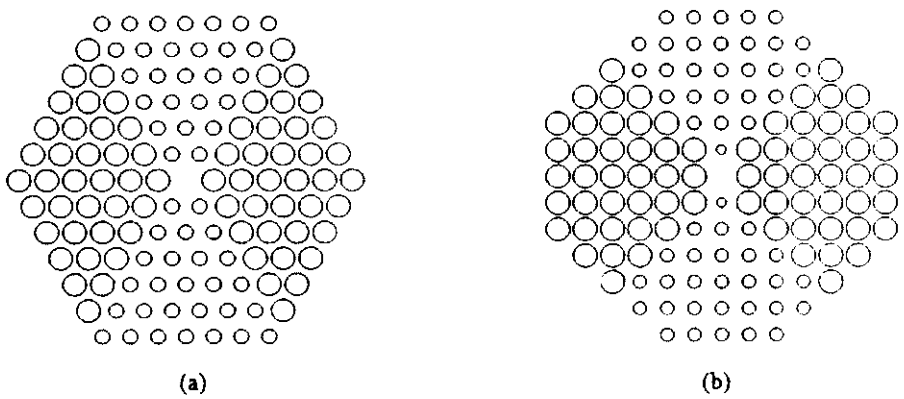

Figure 5.2: cross section of V type PCF with triangular (a) and tetragonal (b) lattice: the radius of the small and the big holes is 0.8 μm, 1.2 μm, respectively

As shown in figure 5.3, the birefringence increases with wavelength, it reaches 1.25 x 10^{-3} around 1.55μm. Both structures have quietly the same evolution.

Figure 5.4 shows the analysis results of the chromatic dispersion. It is clearly displayed that the chromatic dispersion increases strongly with the triangular lattice where it reaches 0.006 ps/nm/km around the 1.55μm. Contrary, it doesn't pass 0.0005 ps/nm/km over the whole used range of wavelength.

The variation of confinement loss is displayed below in figure 5.5. This type of loss starts with values around the zero then it decreases with higher wavelength. The tetragonal lattice and the triangular have almost the same variation with some advantage for this last type where the loss is less high.

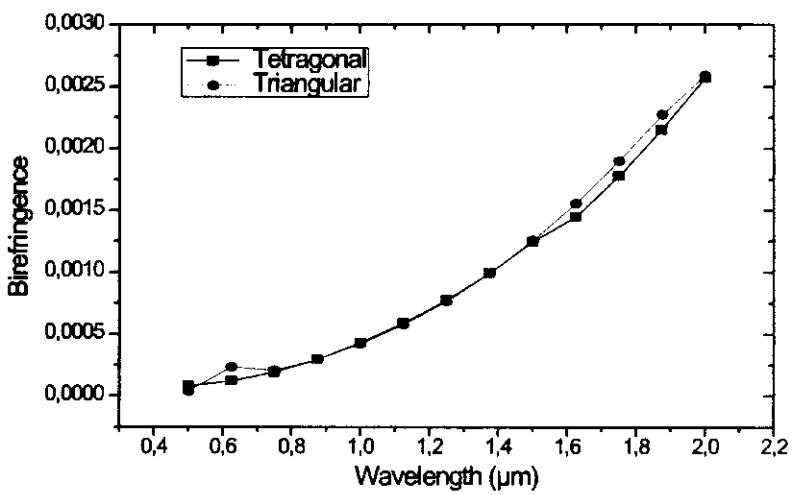

Figure 5.3: evolution of the birefringence with wavelength for the V type PCF

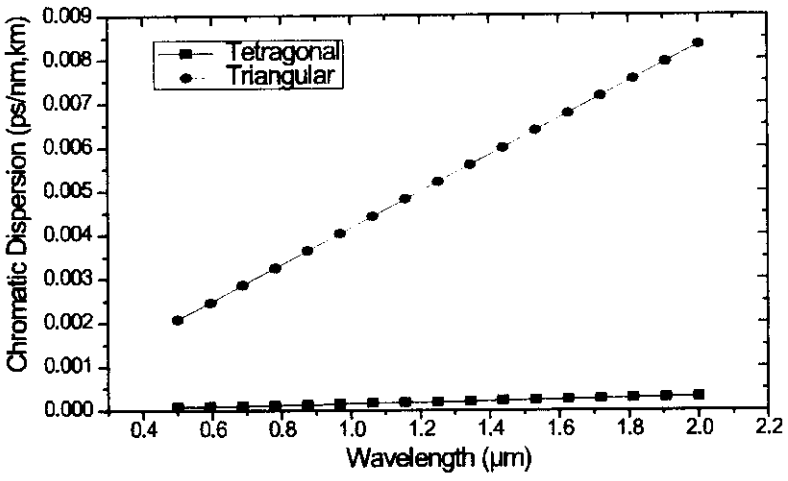

Figure 5.4: evolution of the chromatic dispersion with wavelength for the V type PCF

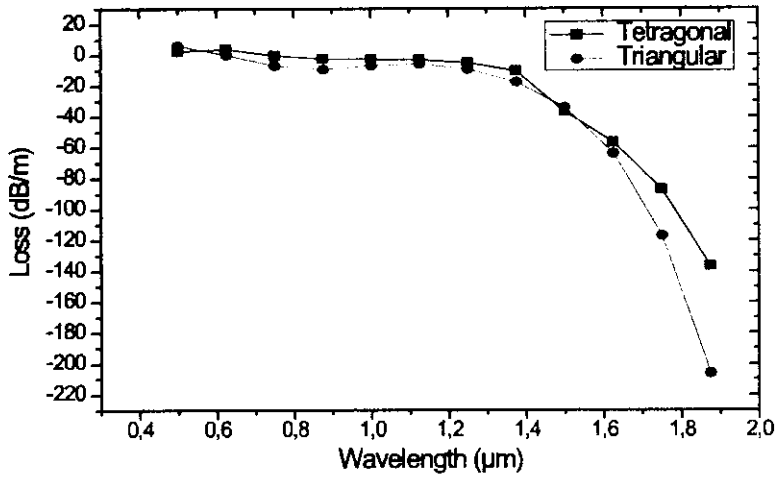

Figure 5.5: evolution of confinement loss with wavelength for the V type PCF

5.4 Pseudo-panda PCF (PP-PCF)

The geometrical structure of the pseudo-panda PCF is illustrated in the figure 5.6. Two enlarged air-holes have been introduced along the x axis between the cladding and the core. The large hole occupies seven small holes in the triangular lattice and six holes in the tetragonal lattice.

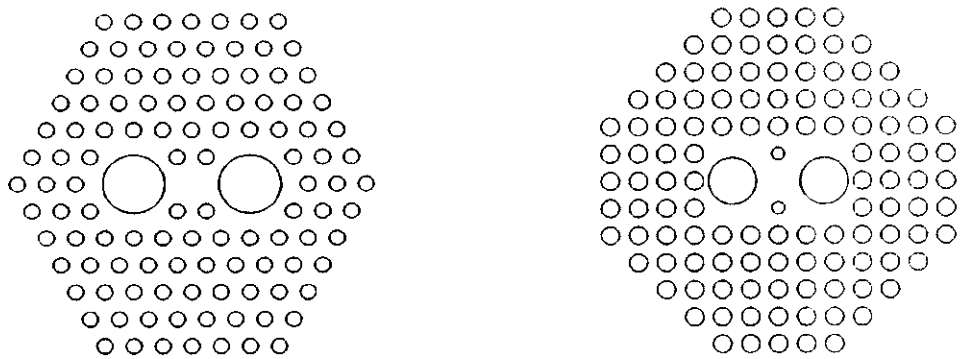

(a) (b)

Figure 5.6: schematic section structure of PP-PCF with triangular (a) and tetragonal (b) lattice

The analysis of this type (figure 5.7) shows that both structures have nearly the same evolution line up to 1.2 μm. For higher wavelengths, the PP-PCF with tetragonal lattice becomes ultra birefringent and reaches the order of magnitude of 10^{-2} (a value of 6 x 10^{-3} of birefringence around 1.55 μm), while it keeps increasing slowly with the triangular lattice.

The figure 5.8 above shows a clearly difference between the two used lattice, the chromatic dispersion is lower when the tetragonal lattice is employed where it doesn't overpass 0.0005 ps/nm/km over the whole used wavelength band, while high values are recorded by the triangular lattice PP-PC.

The evolution of the confinement loss with wavelength as shown below (figure 5.9) displays that the PP-PCF with tetragonal lattice is more efficacy. Both lattices have the same variation up to 0.8 μm, then the loss of tetragonal lattice start decreasing in the same way that the loss of triangular one increasing with. We remark that the value of loss is -150dB/m around 1.55 μm with tetragonal lattice where it 200dB/m with triangular lattice.

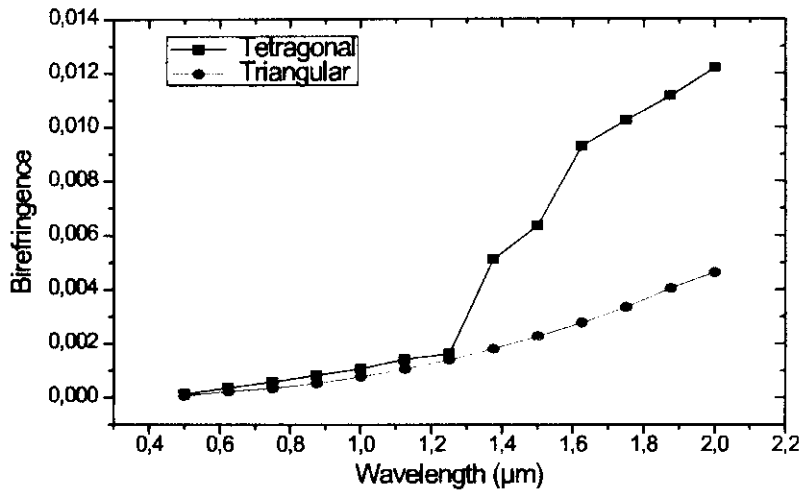

Figure 5.7: evolution of the birefringence with wavelength for the pseudo-panda PCF

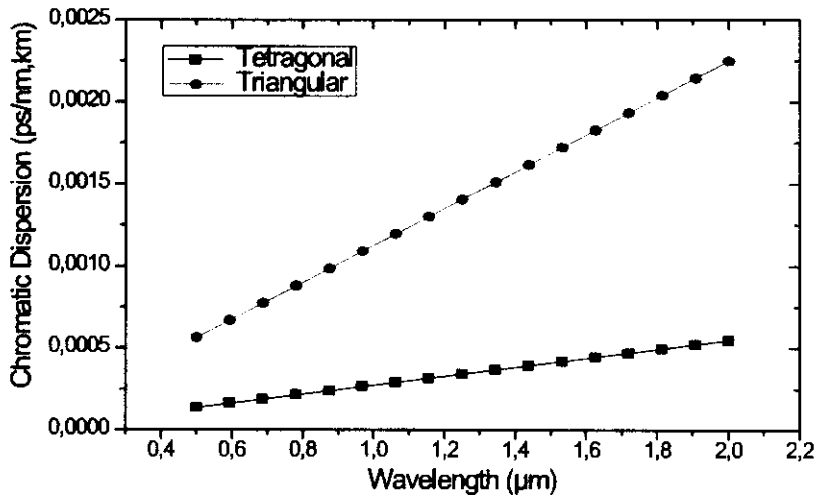

Figure 5.8: evolution of the chromatic dispersion with wavelength for the pseudo-panda PCF

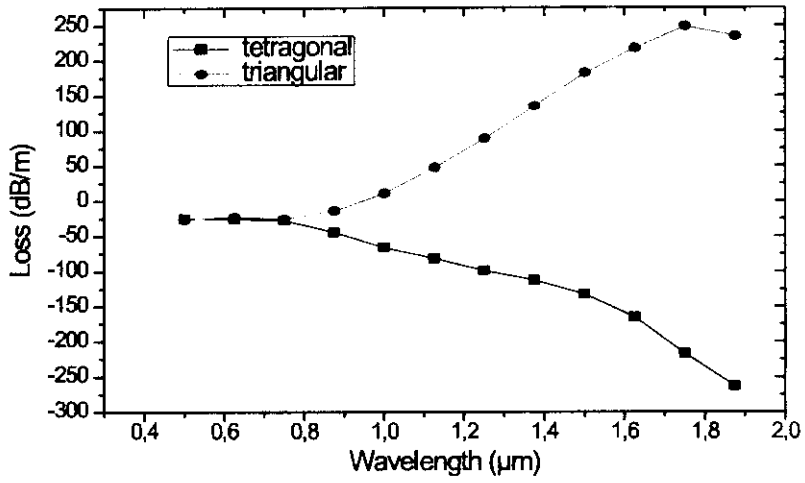

Figure 5.9: evolution of the confinement loss with wavelength for the pseudo-panda PCF

5.5 Selectively liquid-filled PCF

For this case, the birefringence is introduced by infiltrating an index tunable liquid, polymer or opto-fluid into the air-holes of the PCF [97]. The variation of the infiltrated material index can be achieved thermally or electrically [100][106]. Figure 5.10 gives the cross section of such PCF.

The figure 5.11 shows that the birefringence increases with wavelength. Both PCF with tetragonal and triangular lattice have quietly the same evolution with small advantage of the second with wavelengths higher than 1.1 μm.

The evolution of the chromatic dispersion (figure 5.12) displays the clear advantage of the PCF with tetragonal lattice. This is demonstrated by the recorded negative values of chromatic dispersion, also it keeps decreasing with wavelength augmentation to reach higher negative values.

The confinement loss is lower when the tetragonal lattice is used, where it increases slowly up to 1.4 μm to reach the higher value (-50 dB/m) then it starts decreasing strongly. The confinement loss value is -100 dB/km around 1.55 μm for the tetragonal lattice and -60 dB/km for the triangular lattice.

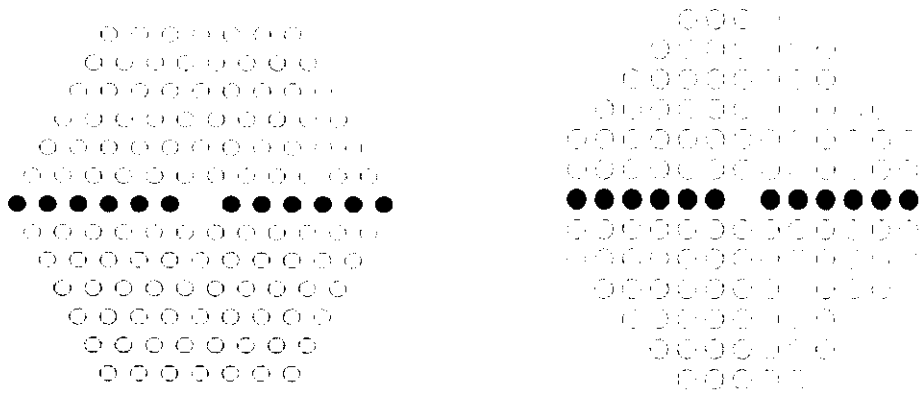

Figure 5.10: schematic section structure of selectively liquid-filled PCF with triangular (a) and tetragonal (b) lattice

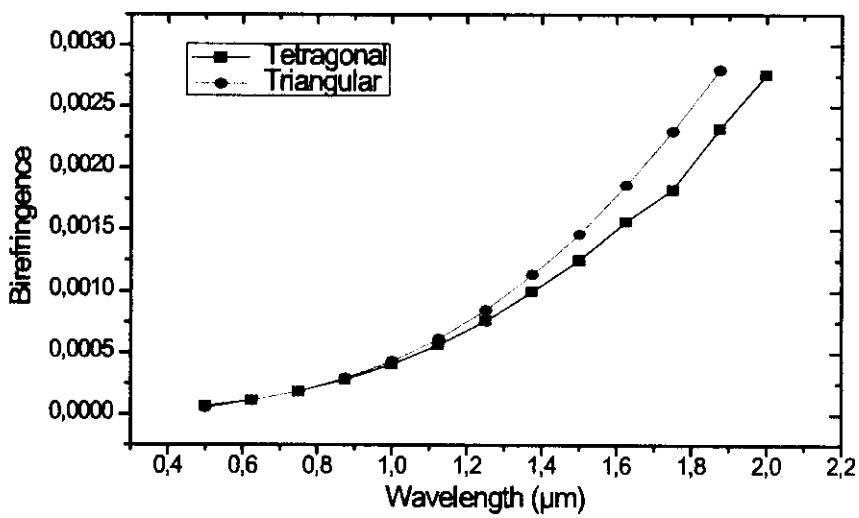

Figure 5.11: evolution of the birefringence with wavelength for the selectively liquid-filled PCF

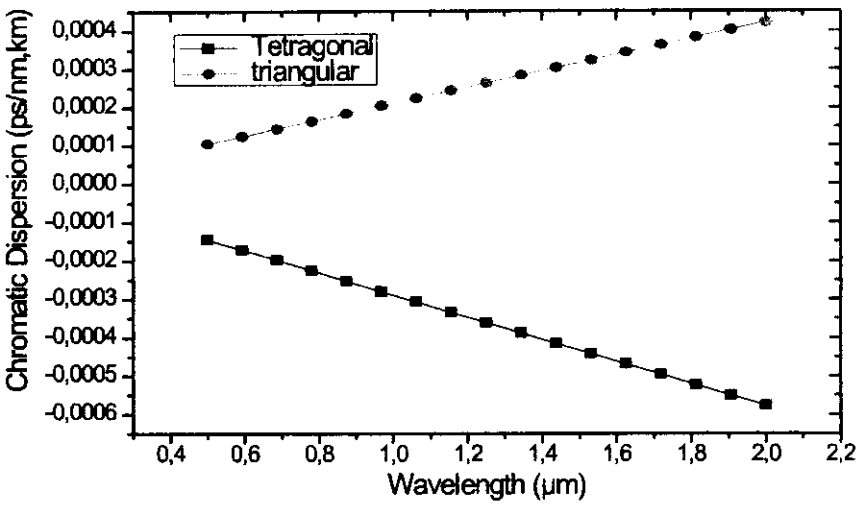

Figure 5.12: evolution of the chromatic dispersion with wavelength for the selectively liquid-filled PCF

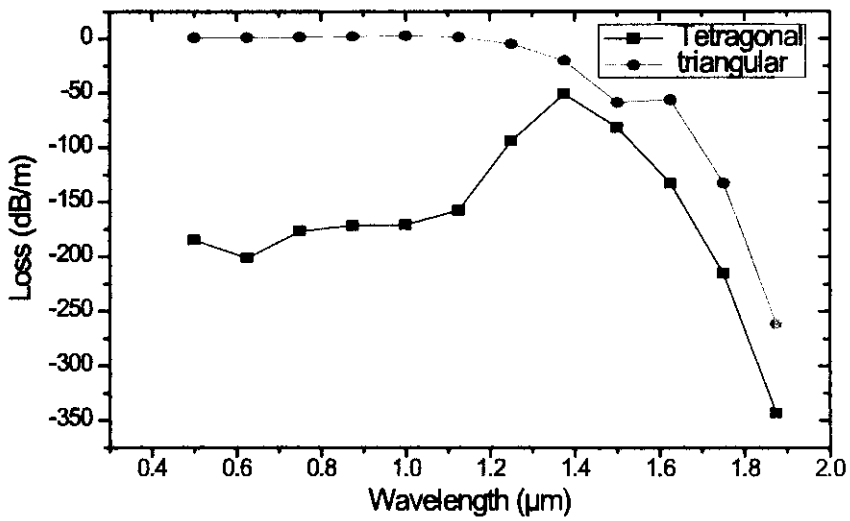

Figure 5.13: evolution of the confinement loss with wavelength for the selectively liquid-filled PCF

5.6 Selectively enlarged air holes PCF

In the design that we are proposing, the PCF is composed of a silica solid core with a refractive index equal to 1.46, surrounded by six rings of circular air holes. The solid core region is formed by removing only one air hole from the center of the structure. The radius of the air holes is 0.7 μm with a pitch (center to center distance between two small air holes) of $\Lambda = 2.5$ μm. The number of rings, which acts as a cladding, is chosen to ensure that the optical field is well confined inside the core, and in such a design the PCF is endlessly single mode [109].

To create the birefringence, the air holes, that are aligned along one axis (the horizontal one in our structure), are differently resized to get a radius larger than all the other air holes [110].

Two lattices are analyzed: a triangular lattice and tetragonal one. Figure 5.14 illustrates the schematic cross section of our model with a triangular lattice (a) and a tetragonal one (b).

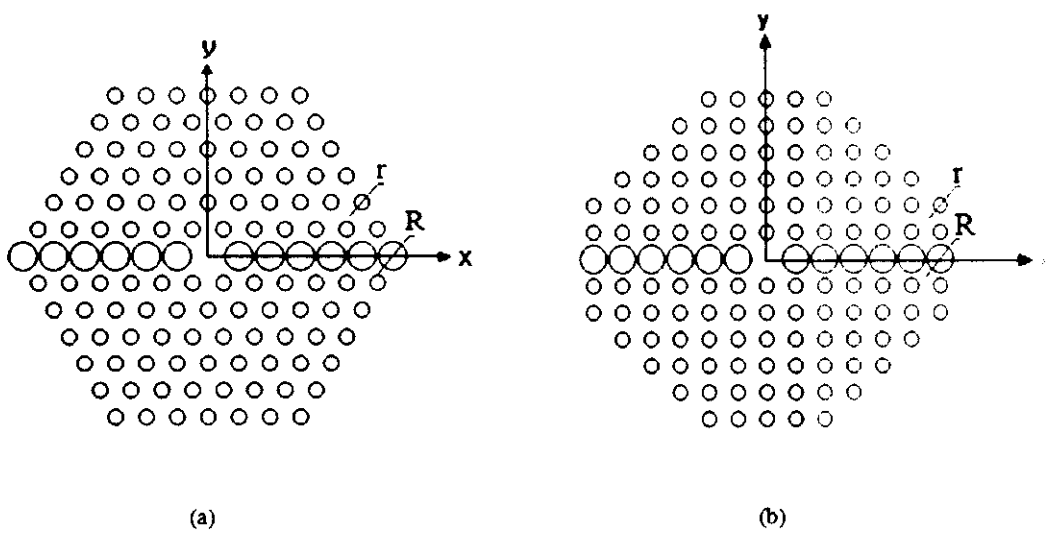

Figure 5.14: schematic section structure of selectively enlarged air holes PCF with triangular (a) and tetragonal (b) lattice

For the triangular lattice, the effective refractive index (n_eff) of the fundamental mode is calculated using the FDTD algorithm. The later is implemented with the Perfectly Matched Layer (PML) boundary condition. Due to the circular symmetry profile, only a quarter of the geometry is the subject of the analysis.

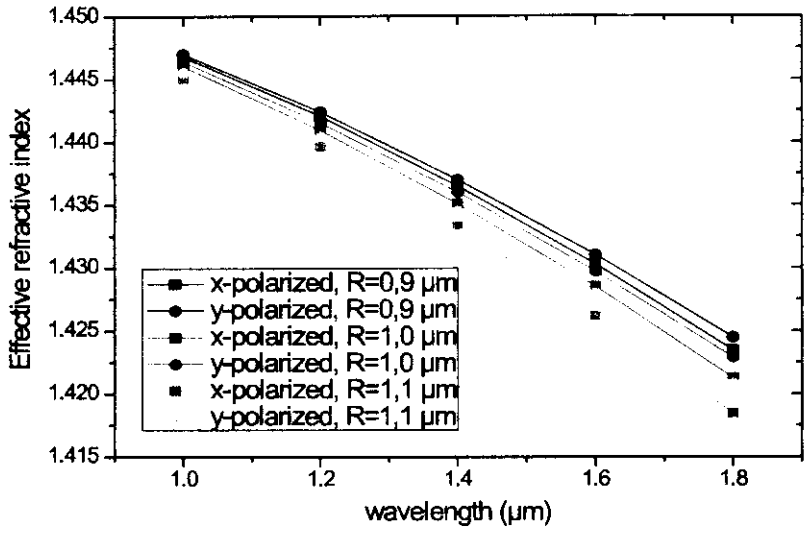

Figure 5.15: evolution of the effective refractive index versus wavelength for different values of the big radius R.

Figure 5.15 gives the evolution of the real part of the effective refractive index as a function of the wavelength. Three values of big air holes radius R are considered: 0.9 μm (D/Λ=0.72), 1 μm (D/Λ=0.8) and 1.1 μm (D/Λ=0.88) with small air holes radius r = 0.7 μm (d/Λ=0.56), where D and d are respectively the diameters of the big and small air holes. The effective index according to y- polarized axis (vertical) has always a larger value than the x-polarized axis (horizontal). Thus, the horizontal axis is faster than the vertical one.

The birefringence is calculated using only the real part of each corresponding effective index. The evolution of the birefringence versus wavelength is illustrated on figure 5.16. Since the birefringence is introduced by enlarging one line of air holes, its value is proportional to the big radius R due to the increasing of air fraction induced stress along this line.

For a wavelength of 1.55 μm and a pitch of 2.5 μm, the birefringence increases from 6 x 10^{-4} for D/Λ=0.72 to 1.55 x 10^{-3} for D/Λ=0.88. This result is quiet the same as what can be obtained if we replace the enlargement procedure by infiltrating a liquid into the air holes as reported by J.-H. Liou et al [111].

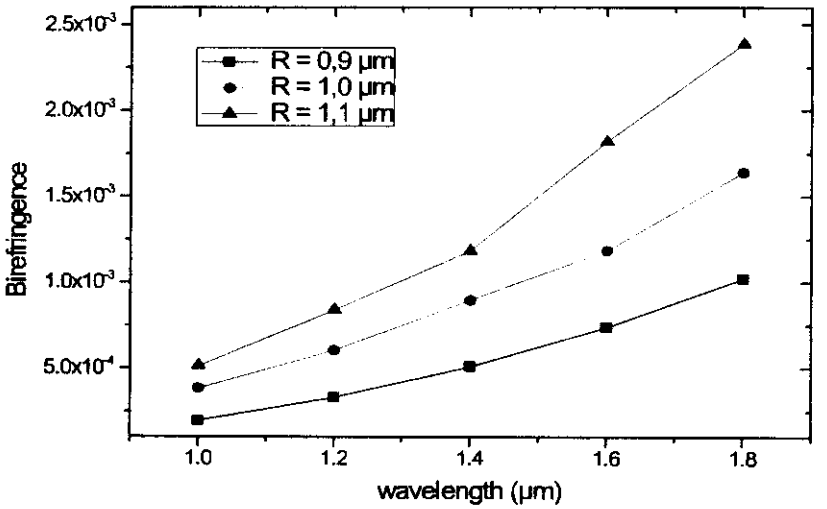

Figure 5.16: evolution of the birefringence versus the wavelength for different values of the big radius R.

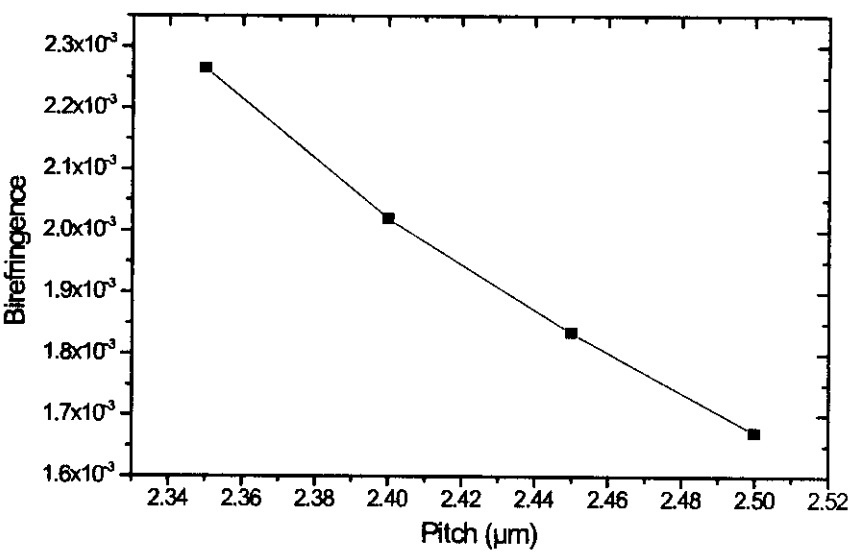

Figure 5.17: evolution of birefringence with the lattice dimension (pitch)

To maximize the birefringence, we studied the effect of the pitch (figure 5.17). As expected, the birefringence increases when the hole to hole spacing decreases. This observation can be explained by the fact that the air fraction induced stress along the horizontal axis increases when the distance between big air holes decreases. For example, with R = 1.1 μm, r = 0.7 μm and Λ=2.35 μm, a birefringence of 2.27 x 10^{-3} can be reached. This result is larger than what is reported in [112][113] and almost equal to what is found by S.S. Mishra et al [114].

Regarding the chromatic dispersion, the simulation was carried out using the geometrical specifications of our design. The evolution of the chromatic dispersion versus wavelength is illustrated on figure 5.18. For D/Λ=0.72 and D/Λ=0.8, the structure is positively dispersive. The dispersion is then flattened with zero value over a band of 1500 nm around the 1.55 μm for D/Λ=0.88 which successfully matches the highest value of birefringence that can be obtained.

The FDTD method is also used to calculate the confinement loss of the fundamental mode. The loss evolution versus wavelength is plotted in figure 5.19. The structure shows a low loss for the entire considered spectral window. For μm the loss level is 0.02 dB/Km, whereas it is equal to 0.2 dB/Km for μm, whatever the value of the big radius R. Such loss is found to be less than what can be obtained if just two air holes are over enlarged along one axis (Pseudo-Panda PCF) [115].

We further studied the geometrical properties of the fundamental mode of our proposed design, when the cladding is formed with a tetragonal lattice of air-holes array. [116][117]. To compare this structure with the first one (triangular lattice PCF), the geometrical parameters are set to be the same, thus, we set D/Λ=0.56 and D/Λ=0.88.

As expected, tetragonal lattice PCF shows a high birefringence due to asymmetric stress induced by the big air holes (figure 5.20). However, triangular lattice PCF shows a birefringence much higher (1.55 x 10^{-3} at the excitation wavelength 1.55 μm) than PCF with tetragonal lattice (0.8 x 10^{-3} at the excitation wavelength 1.55 μm).

On the other hand, and as depicted in figure 5.6, light is guided in tetragonal lattice PCF with very low loss (0.075 dB/Km at the excitation wavelength 1.55 μm) in comparison with triangular lattice PCF (0.17 dB/Km at the excitation wavelength 1.55 μm).

As to the chromatic dispersion, its evolution with wavelength for the two air holes arrays is plotted in figure 5.6. Since the triangular lattice PCF has a zero chromatic dispersion, the tetragonal lattice has a positive dispersion with a very small value, about 4 x 10^{-15} ps/nm.km at the excitation wavelength 1.55 μm.

The analysis presented here, leads to conclude that triangular lattice PCF is preferred because of the appreciable properties that are obtained.

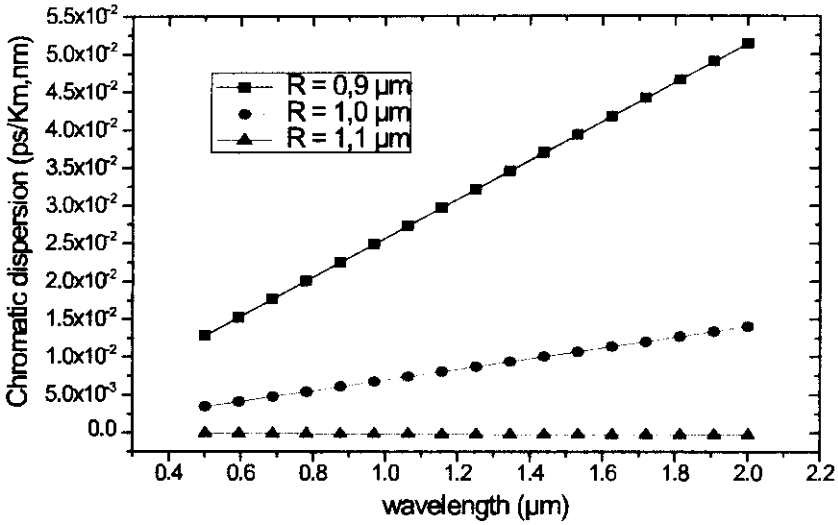

Figure 5.18: evolution of the chromatic dispersion with wavelength for different values of the big radius R

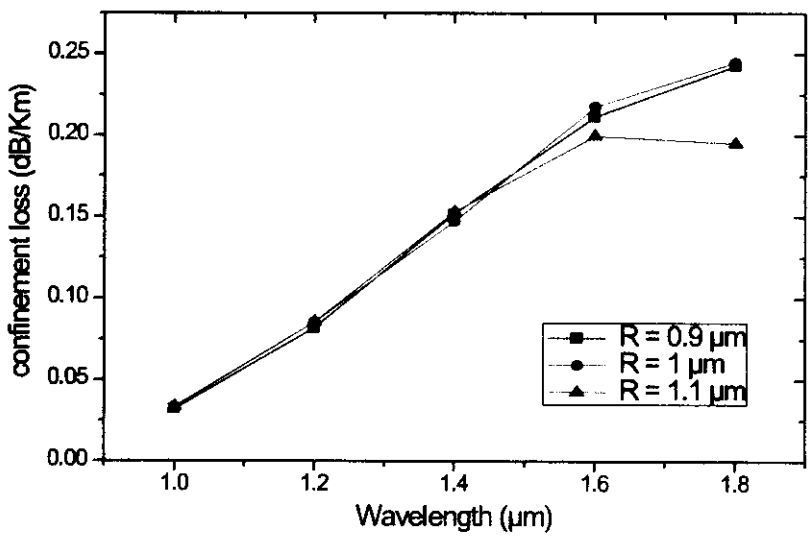

Figure 5.19: evolution of the confinement loss with wavelength for different values of the big radius R.

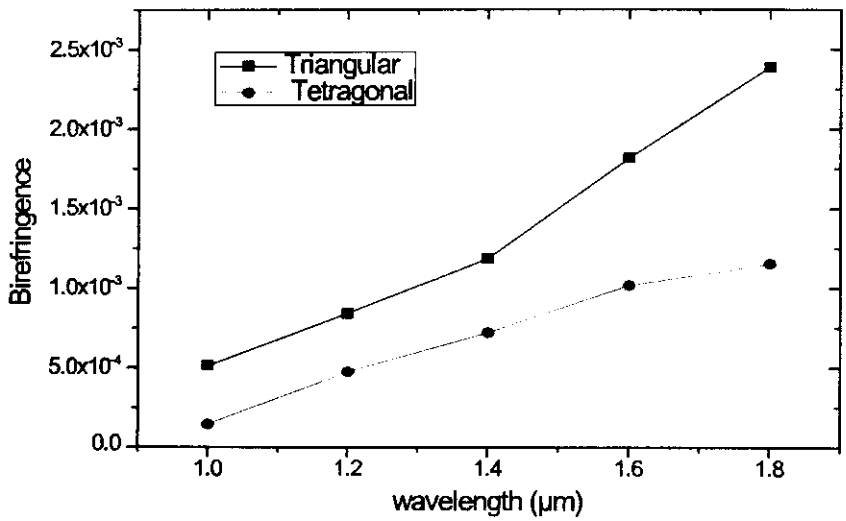

Figure 5.20: evolution of birefringence for PCF with triangular lattice and tetragonal lattice versus wavelength

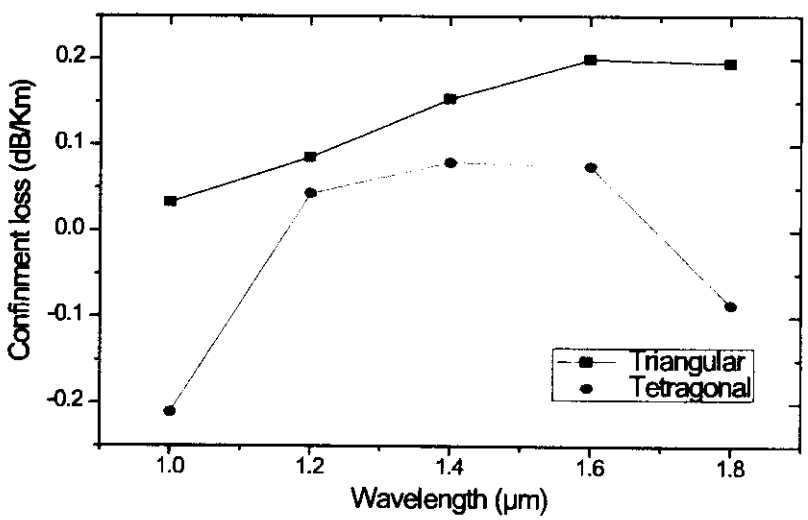

Figure 5.21: evolution of confinement loss for PCF with triangular lattice and tetragonal lattice versus wavelength

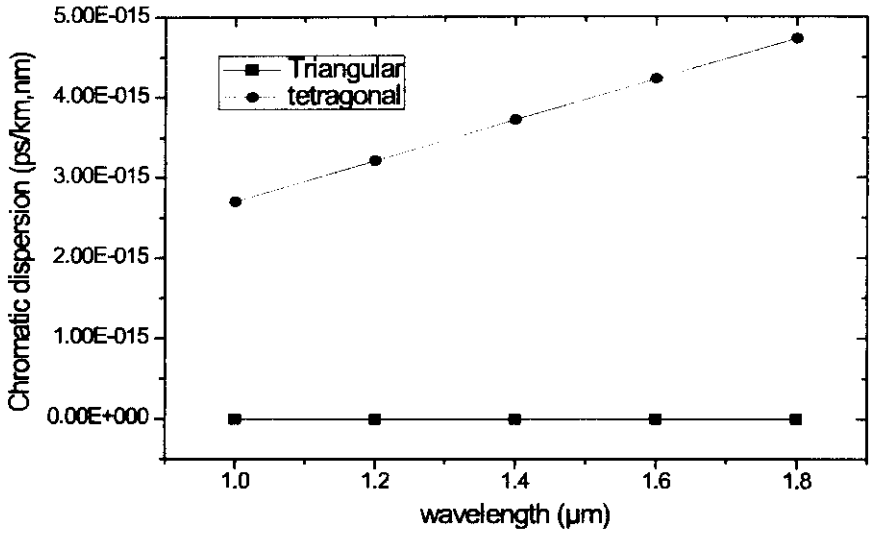

Figure 5.22: evolution of chromatic dispersion for PCF with triangular lattice and tetragonal lattice versus wavelength.

5.7 Conclusion

We numerically studied the mode birefringence, the chromatic dispersion and the confinement loss of four types of high birefringent PCFs by using two lattices in the cladding region based on the FDTD method. For the first three types, it has been found that PCFs with tetragonal lattice are more birefringent whatever the cladding geometry, and a maximum can be obtained with PP-PCF. This advantage is also reinforced by the fact that chromatic dispersion and confinement loss are the both lowest. For the three combined criterions, the PP-PCF with tetragonal lattice is recommended. We had deeply studied the forth type. In the proposed structure, the birefringence is created by resizing the air holes aligned according to one axis to get a radius bigger than the other holes. It has been shown that birefringence can be optimized by enlarging the big air holes or by decreasing the lattice dimension. First, the big radius was 0.9 μm; we obtained a birefringence of around 1.55 μm which is not enough. We have considerably increased the birefringence until for the same wavelength by enlarging the big radius to 1.1 μm with a pitch of 2.5 μm and up to by employing the same radius with a pitch of 2.35 μm. The confinement loss has been found to be 0.17 dB/Km which is very small. We have also successfully optimized the structure parameters and obtained a zero chromatic dispersion for the full wavelength range (small radius of 0.7 μm, big radius of 1.1 μm and a pitch of 2.5 μm). We have also studied the birefringence property of the structure when employing a tetragonal lattice; we have found that it is better to use the triangular one because of the high value of birefringence that can be obtained, whatever the operating wavelength.

General conclusion

The present study aimed at investigating a new design of the optical fiber both theoretically and practically. Extremely unique properties have been provided by the PCF, this latter was the most important application of the two dimensional photonic crystals. In the realm of this study, focus has been given to the linear effects of a solid core PCF applying the well known method finite difference time domain (FDTD). The effective index obtained by the OptiFDTD simulation software, with a complex nature, gave the possibility to prove the endless single mode behavior, and to calculate the chromatic dispersion and birefringence using the real part, also to find the confinement loss using the imaginary part.

A PCF with triangular lattice has been treated to investigate the endless single mode behavior, by varying the diameter of air holes. This fiber has exhibited that it can be monomode over a wide range of wavelengths, where it reached the 1800 nm in the carried experiment. This behavior has also been proved to be related to the air filling fraction and it can be assured by providing a structure with air fraction (d/Λ) less than 0.4.

The discussion of the confinement loss has passed by two steps. The first was as a function of the number of rings that surrounded the core. Manipulating a PCF with high number of rings made the guided mode more confined in the core thus reduced the confinement loss, which is not the case when a less number of air holes layers are provided. The second was the leaky loss as a function of the air holes' size. The structure showed less loss when big size of the air holes was placed; this can be explained by the contrast between the core and the cladding, the refractive index of the latter is affected by the air ratio.

The simulation discussed in this study indicated that the chromatic dispersion can be controlled by the air holes diameter. Using big air holes made the chromatic

dispersion low, and more flattened especially with higher wavelengths, also the zero value of chromatic dispersion was shifted to the operation wavelength 1.55μm every time using bigger air holes.

The geometries of photonic crystal fibers were optimized in order to achieve a high birefringence. This can be obtained by breaking the symmetry between the two orthogonal axes of the fundamental mode. Different patterns have been analyzed: the V-type, the pseudo-panda, and the selectively liquid-filled PCF. A normal structure has been simulated to be as a reference, the birefringence was in order of magnitude of 10^{-4}. The pseudo panda with tetragonal lattice has performed the higher values of birefringence (value of 6 x 10^{-3} of birefringence around 1.55 μm) with less loss and low chromatic dispersion.

Following what precedes, a new design of HI-BI PCF was proposed; the selectively enlarged air holes. The air holes of the horizontal axes have enlarged to reach 1.1 μm. while the rest holes are 0.7 μm with pitch of 2.35μm. This structure is more efficiency comparing with other types since it is hard to fabricate air holes with elliptical form, and also to use the infiltrated liquid because of the fiber length. The obtained birefringence is up to 2.2 x 10^{-3} for the wavelength of 1.55 μm. The corresponding confinement loss is about the 0.17 dB/km. The chromatic dispersion has also optimized to be nil over the wavelength range. The triangular lattice is more compatible with the higher values of birefringence.

Generally, using the high air fraction ratio makes the light more confined in the core, hence the confinement loss becomes small, and the chromatic dispersion flattened and low. On the other hand, this high ratio affects the wavelength band that the PCF is monomode on it. Thus, these parameters must be placed in such a way that keeps the fiber monomode and less loss with low dispersion, or according to the desired purposes (high birefringence, high negative dispersion...).

The domain of photonic crystal fiber "if it can be so-called" is a mysterious world still waiting to be discovered. As for suggestions and future research, non linear effects of the photonic crystal fiber can be discussed. Also, both linear and non linear effects of the hollow core photonic crystal fiber can be studied and investigated. These investigations can be carried out using different numerical methods such as the finite element and the plane wave expansion methods.

Bibliography

[1] E. Yablonovitch, "Inhibited spontaneous emission in solid state physics and electronics," Phys. Rev. Lett., Vol. 58, pp. 2059-2062, 1987

[2] J. G. Maloney, M. P. Kesler, B. L. Shirley, and G. S. Smith, "A simple description for waveguiding in photonic bandgap materials," Microwave Opt. Tech. Lett., Vol. 14, pp. 261-265, 1997.

[3] L. Rayleigh, "On the maintenance of vibrations by forces of double frequency, and on the propagation of waves through a medium endowed with a periodic structure". Philosophical Magazine 24, 145–159 (1887)

[4] V.P. Bykov, "Spontaneous emission in a periodic structure." J. Exp. Theor. Phys. 35, 269 (1972)

[5] E. Yablonovitch, "Inhibited spontaneous emission in solid-state physics and electronics." Phys. Rev. Lett.58, 2059–2062 (1987)

[6] S. John, "Strong localization of photons in certain disordered dielectric superlattices." Phys. Rev. Lett. 58, 2486–2489 (1987)

[7] K.M. Ho, C.T. Chan, C.M. Soukoulis, "Existence of a photonic gap in periodic dielectric structures." Phys. Rev. Lett. 65, 3152–3155 (1990)

[8] H.S. Sozuer, J.W. Haus, R. Inguva, "Photonic bands: Convergence problems with the plane-wave method." Phys. Rev. B45, 13962–13972 (1992)

[9] J.E.G.J. Wijnhoven, L.V. Willem, "Preparation of photonic crystals made of air spheres in Titania." Science 281, 802–804 (1998)

[10] A. Blanco, E. Chomski, S. Grabtchak, et al.," Large-scale synthesis of a silicon photonic crystal with a complete three-dimensional bandgap near 1.5 micrometres." Nature 405 , 437–440 (2000)

[11] J D. Rancourt, "Optical Thin Films User's Handbook". New York: McGraw-Hill (1978)

[12] L.Rayleigh L 1887 "On the maintenance of vibrations by forces of double frequency, and on the propagation of waves through a medium endowed with a periodic structure Phil. Mag.24145

[13] J. Lekner, "Omnidirectional reflection by multilayer dielectric mirrors" J. Opt. A: Pure Appl. Opt. 2 349 (2000)

[14] E. Yablonovitch, "Photonic crystals: what's in a name?" Opt. Photon. News 1812 (2007)

[15] K M. Ho, K M. Chan and C M. Soukoulis, "Existence of a photonic gap in periodic dielectric structures". Phys.Rev. Lett. 653152 (1999)

[16] J B. Pendry and A. MacKinnon, "Calculation of photon dispersion relations" Phys. Rev. Lett.692772 (1992)

[17] J B. Pendry , "Calculating photonic band structure" J. Phys.: Condens. Matter 8 1085 (1996)

[18] J. Arriaga, A J. Ward and J B. Pendry "Order-N photonic band structures for metals and other dispersive materials" Phys. Rev.B 591874 (1999)

[19] P. Vukusic and J R. Sambles, "Photonic structures in biology". Nature 424 852 (2003)

[20] V L. Welch and J-P Vigneron, "Beyond butterflies—the diversity of biological photonic crystals" Opt. Quant. Electron. 39295 (2007)

[21] S. Kinoshita and S. Yoshioka, "Structural colors in nature: the role of regularity and irregularity in the structure" Chem. Phys. Chem. 6 1442 (2005)

[22] Z. Vértesy, ZS. Bàlint, K. Kertész, J P. Vigneron, V. Lousse and L P. Biro, "Wing scale microstructures and nanostructures in butterflies-natural photonic crystals" J. Microsc. 224 108 (2006)

[23] C. Kittel, "Introduction to Solid State Physics" 6th ed, New York: Wiley (1993)

[24] R D. Meade, K D. Brommer, A M. Rappe and J D. Joannopoulos, "Existence of a photonic band gap in two dimensions" Appl. Phys. Lett. 61495. (1992)

[25] E. Yablonovitch, T J. Gmitter and K M. Leung, "Photonic band structure: the face-centered-cubic case employing nonspherical atoms" Phys. Rev. Lett.672295 (1991)

[26] C C. Cheng, V. Arbet-Engels, A. Scherer and E. Yablonovitch, "Nanofabricated three dimensional photonic crystals operating at optical wavelengths". Phys. Scr. T68 17 (1996)

[27] H S. Sozuer and J W. Haus, "Photonic bands: simple-cubic lattice" J. Opt. Soc. Am. B 10296 (1993)

[28] C T. Chan, S. Datta, K M. Ho and C M. Soukoulis, "A7 structure: a family of photonic crystals" Phys. Rev. B 501988 (1994)

[29] K M. Ho, C T. Chan, C M Soukoulis and M. Sigalas, "Photonic band gaps in three dimensions: new layer-by-layer periodic structures" Solid State Electron.89413 (1994)

[30] H S. Sozuer and J P. Dowling, "Photonic band calculations for woodpile structures" J. Mod. Opt.41231 (1994)

[31] E. Ozbay, E. Michel, G. Tuttle, R. Biswas, M. Sigalas and K-M. Ho 1994 "Micromachined millimeter wave photonic band-gap crystals" Appl. Phys. Lett. 642059 (1994)

[32] O. Toader and S. John, "Proposed square spiral microfabrication architecture for large three-dimensional photonic band gap crystals" Science292 1133 (2001)

[33] O. Toader and S. John "Square spiral photonic crystals: robust architecture for microfabrication of materials with large three-dimensional photonic band gaps". Phys. Rev.E 66016610 (2002)

[34] S R. Kennedy, M J. Brett, O. Toader and S. John "Fabrication of square spiral photonic crystals by glancing angle deposition". Proc. SPIE 5023101 (2003)

[35] O. Toader, M. Berciu and S. John, "Photonic band gaps based on tetragonal lattices of slanted pores". Phys. Rev. Lett. 90233901 (2003)

[36] M. Deubel, M. Wegener, A. Kaso, and S. John, "Direct laser writing and characterization of 'Slanted Pore' photonic crystals". Appl. Phys. Lett. 851895 (2004)

[37] P. St. J. Russell and R. Dettmer, "A neat idea [photonic crystal fibre]." IEE Review, vol. 47, pp. 19–23, Sept. 2001.

[38] J. C. Knight, T. A. Birks, P. St. J. Russell, and D. M. Atkin, "Pure silica single-mode fibre with hexagonal photonic crystal cladding," in Proc. Optical Fiber Communications Conference OFC 1996, San Jose, California, USA, Feb. 25 – Mar. 1, 1996.

[39] R. F. Cregan, B. J. Mangan, J. C. Knight, T. A. Birks, P. St. J. Russell, P. J. Roberts, and D. C. Allan, "Single-mode photonic band gap guidance of light in air," Science, vol. 285, pp. 1537–1539, Sept. 1999.

[40] K. Saitoh, M. Koshiba, "Numerical Modeling of Photonic Crystal Fibers", J. of Light. Tech., Vol. 23, N° 11, pp. 3580-3590, 2005.

[41] Web site BLAZEPHOTONICS, http://www.blazephotonics.com/ (26/03/2012)

[42] Web site CRYSTAL FIBRE, http://www.crystal-fibre.com/ (26/03/2012)

[43] Web site REDFERNPOLYMER, http://www.redfernpolymer.com/ (27/03/2012)

[44] P. S. J. Russell, "Photonic-crystal fibers," IEEE Journal of Lightwave Technology 24, pp. 4729-4749, 2006.

[45] P. St. J. Russell, "Photonic crystal fibers," Science, vol. 299, pp. 358–362, Jan. 2003.

[46] J. C. Knight, "Photonic crystal fibres," Nature , vol. 424, pp. 847–851, Aug. 2003.

[47] K. Kurokawa, K. Tajima, K. Tsujikawa, and K. Nakajima, "Reducing the losses in photonic crystal fibres," in Proc. European Conference on Optical Communication ECOC 2005, Glasgow, Scotland, Sept. 25–29, 2005.

[48] D. Ferrarini, L. Vincetti, M. Zoboli, A. Cucinotta, F. Poli, and S. Selleri, "Leakage Losses in Photonic Crystal Fibers," in Proc. Optical Fiber Communications Conference OFC 2003, Atlanta, Georgia, USA, Mar. 23–28, 2003, paper FI5.

[49] J. C. Knight, T. A. Birks, R. F. Cregan, P. St. J. Russell, and J. P. de Sandro, "Large mode area photonic crystal fibre," Electronics Letters , vol. 34, pp. 1347–1348, June 1998.

[50] N. A. Mortensen, M. D. Nielsen, J. R. Folkenberg, A. Petersson, and H. Simonsen, "Improved large-mode-area endlessly single-mode photonic crystal fibers," Optics Letters, vol. 28, pp. 393–395, Mar. 2003.

[51] J. C. Baggett, T. M. Monro, J. R. Hayes, V. Finazzi, and D. J. Richardson, "Improving bending losses in holey fibers," in Proc. Optical Fiber Communications Conference OFC 2005 , Anaheim, California, USA, Mar. 6–11, 2005, paper OWL4.

[52] ITU COM 15-273-E "Definition and Test Methods for the Relevant Parameters of Single-Mode Fibres - Appendix on Nonlinearities for G.650", (1996).

[53] G.P. Agrawal, "Non linear fiber optics", 3rd ed. Academic Press, Boston 2001.

[54] T.M. Monro, D.J. Richardson, "Holey optic al fibres: Fundamental properties and device applications", Comptes Rendues Physique, Vol. 4, pp. 175-186, 2003.

[55] N.A. Mortensen, "Effective area of photonic crystal fi bers", Opt. Exp., Vol. 10, N° 7, pp. 341-348, 2002.

[56] A. Bjarkiev, J. Broeng, AS Bjarkiev, "Photonic crystal fibers", Kluwer Accedemic Publishers, (2003).

[57] J. C. Knight, T. A. Birks, P. S. J. Russell and D. M. Atkin, "All-silica single-mode optical fiber with photonic crystal cladding", Optics Lett. 21 (19), pp.1547,(1996).

[58] B. Bourliaguet, C. Paré, "Applications des fibres microstructurées", web site : ofl.phys.polymtl.ca/ogp8/c/Bourliaguet_c.pdf.

[59] L.P. Shen, W.P. Huang, G.X. Chen, S.S. Jian, "Design and optimization of photonic crystal fibers for broad-band dispersion comp ensation", Photon. Tech. Lett., Vol. 15, N° 4, pp. 540-542, 2003.

[60] K. Saitoh, M. Koshiba T. Hasegawa, E. Sasaoka, "Chromatic dispersion control in photonic crystal fibers: application to ultra-flattened di spersion", Opt. Exp., Vol. 11, N° 8, pp. 843-852, 2003.

[61] A. Huttunen, P. Toma, "Optimization of dua l-core and microstructure fiber geometries for dispersion compensation and large mode area", Opt. Exp., Vol. 13, N° 2, pp. 627-635, 2005.

[62] A. Ferrando, E. Silvestre, P. Andres, J.J. Miret, M.A. Andres, "Designing the properties of dispersion-flattened photonic crystal fibers", Opt. Exp., Vol. 9, N° 13, pp.687-697, 2001.

[63] W.H. Reeves, J.C. Knight, P.St.J. Russell, P.J. Roberts, "Demonstration of ultra-flattened dispersion in photonic crystal fibers", Opt. Exp., Vol. 10. N° 14, pp. 609-613, 2002.

[64] J. Limpert, T. Schreiber, S. Nolte, H. Zellmer, A. Tunnermann, R. Iliew, F. Lederer, J. Broeng, G. Vienne, A. Petersson, and C. Jakobsen,"High-powerair-cladlarge-mode-areaphotoniccrystal fiberlaser," Opt.Expr.,vol. 11, pp. 818-823,2003.

[65] E. Snitzer, H. Po, F. Hakimi, R. Tumminelli, and B. C. McCollum, "Double Clad, Offset Core Nd Fiber Laser" Optical Fiber Sensors Conference, PD 5 (New Orleans, 1988).

[66] W. N. MacPherson et al. , Opt. Commun. 193, 97 (2001)

[67] T. M. Monro, W. Belardi, K. Furusawa, J. C. Baggett, N. G. R. Broderick, and D. J. Richardson, Meas. Sci. Technol. 12, 854 (2001).

[68] VENGSARKAR, A.M., LEMAIRE, P.J., JUDKINS, J.B., BHATIA, V., ERDOGAN, T., and SIPE, J.E.: 'Long-period fiber gratings as band rejection filters', J. Lightwave Technol., 1996, 14, pp. 58-64

[69] KAKARANTZAS, G., BIRKS, T.A., and RUSSELL, P.St.J.: 'Structural long-period gratings in photonic crystal fibers', Opt. Lett., 2002, 27, pp 1013-1015

[70] MALKI, A., HUMBERT, G., OUERDANE, Y., BOUKHENTER, A., and BOUDRIOUA, A.: 'Investigation of the writing mechanism of electric-arc-induced long-period fiber gratings', Appl. Opt., 2003, 42, pp 3776-3779

[71] B. J. Mangan, J. Arriaga, T. A. Birks, J. C. Knight, and P. St. J. Russell, Opt. Lett. 26, 1469 (2001)

[72] B. J. Eggleton, C. Kerbage, P. S. Westbrook, R. S. Windeler, and A. Hale. Opt. Express9, 698 (2001)

[73] T. A. Birks, D. M. Atkin, G. Wylangowski, P. St. J. Russell, and P. J. Roberts, "2D photonic band gap structures in fibre form," in Photonic Band Gap Materials, C. M. Soukoulis (ed.) Dordrecht: Kluwer, 1996, pp. 437–444.

[74] J. Lœgsgaard and A. Bjarklev, "Microstructured optical fibers – funda-mentals and applications," Journal of the American Ceramic Society, vol. 89, pp. 1–12, Jan. 2006

[75] D.C. Allan et al, in Photonic Crystals and light localization in the 21st Century, C. M. Soukoulis, Ed., pg 305, Kluwer, Netherlands (2001).

[76] K. M. Kiang, K.Frampton, T. M. Monro, R. Moore, J. Tucknott, D.W. Hewak, D. J. Richardson and H. N. Rutt, " Extruded singlemode non-silica glass holey optical fibers", Electronics Letters 38, 546-547 (2002).

[77] J. S. Wang, E. M. Vogel and E. Snitzer, "Tellurite glass: a new candidate for fiber devices", Optical Materials 3, 187-203 (1994).

[78] T.A. Birks, J.C. Knight, and P.S.J. Ru ssell, "Endlessly single-mode photonic crystal fiber," Optics Lett., Vol. 22, No. 13, pp. 961-963, 1997.

[79] Ferrando, A., E. Silvestre, J. J. Miret, and P. Andres, "Nearly zero ultra flattened dispersion in photonic crystal fibers," Opt. Lett.,Vol. 25, 790-792, 2000.

[80] Poletti F., V. Finazzi, T. M. Monro, N. G. R. Broderick, V. Tse, and D. J. Richardson, "Inverse design and fabrication tolerances of ultra-flattened dispersion holey fibers", Opt. Express, Vol. 13, 3728-3736, 2005.

[81] Gérome, F., J.-L. Auguste, and J.-M. Blondy, "Design of dispersion-compensating fibers based on a dual-concentric-core photonic crystal fiber", Opt. Lett., Vol. 29, 2725-2727, 2004

[82] Yang, S., Y. Zhang, X. Peng, Y. Lu, S. Xie, J. Li, W. Chen, Z. Jiang, J. Peng, and H. Li, "Theoretical study and experimental fabrication of high negative dispersion photonic crystal fiber with large area mode field," Opt. Express, Vol. 14, 3015-3023, 2006.

[83] [4.1] T. A. Birks, J. C. Knight, and P. St. J. Russell, Opt. Lett. 22, 961-963 (1997).

[84] Roberts et al, J. Opt. Fiber. Commun. Rep. 2, 435–461 (2005)

[85] J. C. Knight, T. A. Birks, R. F. Cregan, P. St. J. Russel, and J. –P. de Sandro, Electron. Lett. 34, 1347-1348 (1998).

[86] Shen, G.-F., X.-M. Zhang, H. Chi, and X.-F. Jin, Progress In Electromagnetics Research, Vol. 80, 307-320, 2008.

[87] Nozhat, N. and N. Granpayeh, Progress In Electromagnetics Research, Vol. 99, 225-244, 2009.

[88] Chau et al. Progress In Electromagnetics Research B, Vol. 22, 39-52, 2010.

[89] Y.-S. SUN et al. Japanese Journal of Applied Physics. Vol. 47, No. 5, 2008, pp. 3755–3759.

[90] X. Zhang, J. Zhao, Nucl. Instr. and Meth. A (2010), doi:10.1016/j.nima.2010.02.037.

[91] Yue, Y., G. Kai, Z. Wang, T. Sun, L. Jin, Y. Lu, C. Zhang, Opt. Lett., Vol. 32, 469-471, 2007

[92] J. Liu, Y. Li, Y. Liu, S. Yuan, and X. Dong, Opt. Lett., Vol. 32, 469-471, 2007.

[93] Steel, M. J. and R. M. Osgood, Jr., Opt. Lett., Vol. 26, 229-231, 2001.

[94] Chen, D. and L. Shen, " IEEE Photon. Technol. Lett., Vol. 19, 185-187, 2007.

[95] M. J. Steel and R. M. Osgood: J. Lightwave Technol. 19 (2001) 495.

[96] K. Saitoh and M. Koshiba: IEEE Photonics Technol. Lett. 14 (2002)1291.

[97] A. Hochman and Y. Leviatan: Opt. Express 13 (2005) 6193.

[98] J.-H. Liou et al. Optics Communications 283 (2010) 971–974.

[99] J. Wojcik, et al, PHOTONICS LETTERS OF POLAND, VOL. 2 (1), 10-12 (2010).

[100] S. ERTMAN et al. OptoElectron. Rev., 17, no. 2, 2009.

[101] C. Kerbage, P. Steinvurzel, P. Reyes, P.S. Westbrook, R.S. Windeler, A. Hale, B.J. Eggleton, Opt. Lett. 27 (2002) 158.

[102] C. Kerbage, P. Steinvurzel, A. Hale, R.S.Windeler, B.J. Eggleton, Electron. Lett. 38 (2002) 310.

[103] B.J. Eggleton, C. Kerbage, P.S. Westbrook, R.S. Windeler, A. Hale, Opt. Express 9 (2001) 698.

[104] D.C. Zografopoulos, E.E. Kriezis, T.D. Tsiboukis, Opt. Express 14 (2006) 914.

[105] T.R. Wolinski, A. Czapla, S. Ertman, M. Tefelska, A.W. Domaı´ski, E. Nowinowski-Kruszelnicki, R. Dàbrowski, Opt. Quant. Electron. 39 (2007) 1021.

[106] C. Monat, P. Domachuk, C. Grillet, M. Collins, B.J. Eggleton, M. Cronin-Golomb, S. Mutzenich, T. Mahmud, G. Rosengarten, A. Mitchell, Microfluid. Nanofluid. 4 (2008) 81.

[107] B.T. Kuhlmey, B.J. Eggleton, D.K.C. Wu, J. Lightwave Technol. 27 (2009) 1617.

[108] J. Wang et al. Optics & Laser Technology 39 (2007) 317–321.

[109] F. Poli A. Cucinotta S. Selleri, "Photonic Crystal Fibers, Properties and Applications", Springer, 2007.

[110] Lina He, Yejin Zhang, Sigang Yang, Xiangfei Chen, and Shizhong Xie, Microwave And Optical Technology Letters / Vol. 48, No. 5, 2006.

[111] Kubota, H., S. Kawanishi, S. Koyanagi, M. Tanaka, and S. Yamaguchi, IEEE Photon. Technol. Lett.16 (2004) 182-184.

[112] S.P. Guo, F. Wu, S. Albin, Opt. Express. 12 (2004) 3341.

[113] [4.31] Jia-Hong Liou, Sheng-Shuo Huang, Chin-Ping Yu, Optics Communications. 283 (2010) 971–974.

[114] S.S. Mishra et. al, International Journal of Engineering Science and Technology. Vol. 2(9), (2010), 4520-4525

[115] J Olszewski, J. Opt. A: Pure Appl. Opt. 11 (2009).

[116] Arismar Cerqueira S Jr, Rep. Prog. Phys. 73 (2010) 024401.

[117] Couny F, Roberts P J, Benabid F and Birks T A ,Proc. Conf. on Lasers and Electro-Optics (Baltimore, MD), 2008.